JCI The Journal of Clinical Investigation

RASA1-dependent cellular export of collagen IV controls blood and lymphatic vascular development

Di Chen, … , Philip E. Lapinski, Philip D. King

J Clin Invest. 2019. https://doi.org/10.1172/JCI124917.

Research In-Press Preview **Angiogenesis** **Vascular biology**

Combined germline and somatic second hit inactivating mutations of the*RASA1* gene, which encodes a negative regulator of the Ras signaling pathway, cause blood and lymphatic vascular lesions in the human autosomal dominant vascular disorder capillary malformation-arteriovenous malformation (CM-AVM). How *RASA1* mutations in endothelial cells (EC) result in vascular lesions in CM-AVM is unknown. Here, using different murine models of RASA1-deficiency, we found that RASA1 was essential for the survival of EC during developmental angiogenesis in which primitive vascular plexuses are remodeled into hierarchical vascular networks. RASA1 was required for EC survival during developmental angiogenesis because it was necessary for export of collagen IV from EC and deposition in vascular basement membranes. In the absence of RASA1, dysregulated Ras mitogen-activated protein kinase (MAPK) signal transduction in EC resulted in impaired folding of collagen IV and its retention in the endoplasmic reticulum (ER) leading to EC death. Remarkably, the chemical chaperone, 4-phenylbutyric acid, and small molecule inhibitors of MAPK and 2-oxoglutarate dependent collagen IV modifying enzymes rescued ER retention of collagen IV and EC apoptosis and resulted in normal developmental angiogenesis. These findings have important implications with regards an understanding of the molecular pathogenesis of CM-AVM and possible means of treatment.

RASA1-dependent cellular export of collagen IV controls blood and lymphatic vascular development

Di Chen[1], Joyce Teng[2], Paula North[3], Philip E. Lapinski[1], and Philip D. King[1]

[1]Department of Microbiology and Immunology, University of Michigan Medical School, Ann Arbor, Michigan, USA

[2]Department of Dermatology, Stanford University, Stanford, California, USA

[3]Department of Pathology, Medical College of Wisconsin, Children's Hospital of Wisconsin, Milwaukee, Wisconsin, USA

Correspondence:
Philip D. King
Department of Microbiology and Immunology
University of Michigan Medical School
6606 Med Sci II
1150 West Medical Center Drive
Ann Arbor
MI 48109-5620
Tel: 734-615-9073
Fax: 734-764-3562
E-mail: kingp@umich.edu

Conflict of interest statement: The authors have declared that no conflict of interest exists

Combined germline and somatic second hit inactivating mutations of the *RASA1* gene, which encodes a negative regulator of the Ras signaling pathway, cause blood and lymphatic vascular lesions in the human autosomal dominant vascular disorder capillary malformation-arteriovenous malformation (CM-AVM). How *RASA1* mutations in endothelial cells (EC) result in vascular lesions in CM-AVM is unknown. Here, using different murine models of RASA1-deficiency, we found that RASA1 was essential for the survival of EC during developmental angiogenesis in which primitive vascular plexuses are remodeled into hierarchical vascular networks. RASA1 was required for EC survival during developmental angiogenesis because it was necessary for export of collagen IV from EC and deposition in vascular basement membranes. In the absence of RASA1, dysregulated Ras mitogen-activated protein kinase (MAPK) signal transduction in EC resulted in impaired folding of collagen IV and its retention in the endoplasmic reticulum (ER) leading to EC death. Remarkably, the chemical chaperone, 4-phenylbutyric acid, and small molecule inhibitors of MAPK and 2-oxoglutarate dependent collagen IV modifying enzymes rescued ER retention of collagen IV and EC apoptosis and resulted in normal developmental angiogenesis. These findings have important implications with regards an understanding of the molecular pathogenesis of CM-AVM and possible means of treatment.

Introduction

Capillary malformation-arteriovenous malformation (CM-AVM) is an autosomal dominant inherited vascular disease that is characterized by one or more cutaneous CM together with fast flow vascular lesions in one third of patients (1-3). Fast flow lesions, which include AVMs and arteriovenous fistulas, occur in different anatomical locations and can be life-threatening. Lymphatic vessel (LV) abnormalities that result in lymphedema, chylothorax and chylous ascites have also been identified in a minority of CM-AVM patients (2-7). In the majority of CM-AVM cases, blood vessel (BV) and LV lesions are present at birth, although can also develop throughout childhood and up to early adulthood.

Inactivating germline mutations of the *RASA1* gene are responsible for approximately fifty percent of CM-AVM cases (1-3). *RASA1* encodes p120 Ras GTPase-activating protein (p120 RasGAP or RASA1), a negative-regulator of the Ras small GTP-binding protein that promotes cell growth, proliferation and differentiation (8-10). In quiescent cells, Ras exists predominantly in an inactive GDP-bound state. Growth factors promote the conversion of Ras to an active GTP-bound state that results in the triggering of downstream signaling pathways including the mitogen-activated protein kinase (MAPK) and phosphatidylinositol 3-kinase (PI3K) pathways that drive cellular responses. RASA1 inhibits Ras signal transduction by augmenting the ability of Ras to hydrolyze bound GTP resulting in its conversion to the inactive GDP-bound form (8). Vascular lesions in CM-AVM patients with germline *RASA1* mutations arise as a consequence of somatic inactivating mutation of the inherited wild-type *RASA1* allele in endothelial cells (EC) or

their precursors (6, 11). Loss of RASA1 in these EC would be expected to result in dysregulated Ras signal transduction that could drive lesion development.

Recently, it has been shown that inactivating germline mutations of *EPHB4*, which encodes the ephrin receptor B4, are responsible for the majority of CM-AVM cases that are not explained by *RASA1* mutation (12). Accordingly, CM-AVM resulting from *RASA1* mutation has been re-named CM-AVM1 and CM-AVM resulting from *EPHB4* mutation has been named CM-AVM2. Clinically, CM-AVM1 and CM-AVM2 are almost indistinguishable except for the additional occurrence of telangiectasias in CM-AVM2 (12). These findings raise the possibility that lesion development in CM-AVM results from loss of an EPHB4-RASA1 negative-regulatory axis in EC in which EPHB4 serves to recruit RASA1 to the inner leaflet of the cell membrane allowing its juxtaposition to Ras-GTP (12, 13). It is likely that second hit mutations of *EPHB4* are required for the development of lesions in CM-AVM2, although this has yet to be demonstrated.

Studies of genetically engineered mutant mice have the potential to provide information upon the pathogenesis of diseases such as CM-AVM that could not otherwise be obtained from human studies alone. Concerning *RASA1* and CM-AVM1, constitutive loss of *Rasa1* in mice results in mid-gestation lethality at E10.5 as a consequence of impaired vascular development (14, 15). Developmental angiogenesis, in which primitive vascular plexuses are remodeled into hierarchical vascular networks, is abnormal in these embryos. This is evident in the yolk sac for example where EC initially assemble into a vascular plexus but then fail to organize into a vascular network that supplies blood to the

developing embryo. Some defects in vasculogenesis are also evident in RASA1-deficient embryos. In contrast to this, in adults, induced global disruption of *Rasa1* does not result in any spontaneous BV abnormalities (16). Instead, mice develop LV hyperplasia and leakage that results in chylous ascites and chylothorax (16). Recently, we demonstrated that RASA1 is essential for the development and maintenance of valves in collecting LV which accounts for LV leakage in the absence of RASA1 (17).

To further understand the role of RASA1 in the BV and LV systems and how its loss may contribute to the vascular phenotypes observed in CM-AVM1, in the current study, we examined the influence of embryonic loss of RASA1 after E10.5. By E10.5, vasculogenesis, is largely complete and the remainder of vascular development is devoted to remodeling of the vascular network by angiogenic processes (18). RASA1 was found to be essential for continued vascular development during this period by promoting the survival of EC. Unexpectedly, the pro-survival function of RASA1 in EC during developmental angiogenesis could be explained on the grounds that it is required for the proper folding and export from EC and vascular smooth muscle cells (VSMC) of collagen IV, a major constituent of vascular basement membranes (BM). We show further that RASA1 is required for normal retinal angiogenesis in newborns and pathological angiogenesis in adults and that this is again most likely explained by its role in the export of collagen IV for deposition in BM. These findings reveal a previously unappreciated role for RASA1 in vascular biology and are of relevance to an understanding of the pathogenesis and treatment of CM-AVM.

Results

Global disruption of Rasa1 during developmental angiogenesis results in hemorrhage, edema and EC apoptosis. To examine the influence of global RASA1 loss upon developmental angiogenesis, we administered tamoxifen (TM) to pregnant *Rasa1*$^{fl/fl}$ mice carrying *Rasa1*$^{fl/fl}$ and *Rasa1*$^{fl/fl}$ *Ub*^{ert2cre} embryos at E12.5-E14.5. Administration of TM to *Rasa1*$^{fl/fl}$ *Ub*^{ert2cre} embryos at this time resulted in visible cutaneous hemorrhage and an edematous appearance at E18.5-E19.5 (Table 1 and Figure 1A). Histological analysis of embryos revealed extravasated erythrocytes in skin associated with damaged cutaneous BV and a vastly reduced number of cutaneous LV (Figure 1A). The same phenotypes were not observed in *Rasa1*$^{fl/fl}$ *Ub*^{ert2cre} embryos that were not administered TM (Supplemental Figure 1A). Administration of TM to *Rasa1*$^{fl/fl}$ *Ub*^{ert2cre} embryos at E15.5 and later also did not result in hemorrhage or other spontaneous embryonic BV abnormalities, although does result in failed LV valve development as we reported previously (17).

Failed LV valve development in embryos administered TM at E15.5 is explained by apoptosis of LV endothelial cells (LEC) in developing LV valve leaflets (17). Therefore, we asked if disruption of *Rasa1* in *Rasa1*$^{fl/fl}$ *Ub*^{ert2cre} embryos before E15.5 induced apoptosis of BV endothelial cells (BEC) and LEC in BV and LV walls. As revealed by immunostaining for activated caspase 3, apoptotic BEC were identified in the vast majority of cutaneous BV of *Rasa1*$^{fl/fl}$ *Ub*^{ert2cre} embryos that were administered TM between E12.5 and E14.5 as determined at E18.5-E19.5 (Figure 1B) but not in *Rasa1*$^{fl/fl}$ *Ub*^{ert2cre} embryos that did not receive TM (Supplemental Figure 1B). Likewise, within the

few LV that could be identified in these embryos at these times, apoptotic LEC were frequently observed (Supplemental Figure 2). Apoptosis of BEC and LEC, therefore, is likely to contribute to hemorrhage and edema in *Rasa1*$^{fl/fl}$ *Ub*^{ert2cre} embryos administered TM between E12.5 and E14.5.

Disruption of Rasa1 specifically within EC is sufficient for EC apoptosis during developmental angiogenesis. To determine if the vascular abnormalities observed in *Rasa1*$^{fl/fl}$ *Ub*^{ert2cre} embryos treated with TM between E12.5 and E14.5 were a consequence of loss of RASA1 within EC themselves, we performed similar experiments using an EC-specific *Cdh5*^{ert2cre} driver (19). Pregnant *Rasa1*$^{fl/fl}$ mice carrying *Rasa1*$^{fl/fl}$ and *Rasa1*$^{fl/fl}$ *Cdh5*^{ert2cre} embryos were administered TM at E13.5 and harvested at E18.5 or E19.5, i.e. 5 or 6 days later respectively. At E18.5, cutaneous hemorrhage was observed in TM-treated but not untreated *Rasa1*$^{fl/fl}$ *Cdh5*^{ert2cre} embryos, which was confirmed by histological analysis (Table 1, Figure 2A and Supplemental Figure 3A). However, hemorrhage was more localized in *Rasa1*$^{fl/fl}$ *Cdh5*^{ert2cre} embryos than in *Rasa1*$^{fl/fl}$ *Ub*^{ert2cre} embryos at this time (compare Figure 1A). In contrast, at E19.5, extensive hemorrhage and edema was observed in *Rasa1*$^{fl/fl}$ *Cdh5*^{ert2cre} embryos (Table 1 and Figure 2B). Furthermore, apoptotic BEC were readily observed in BV of *Rasa1*$^{fl/fl}$ *Cdh5*^{ert2cre} embryos at E19.5 (Figure 2C) but not E18.5 (see later). As shown by real time qPCR analysis of sorted skin BEC from TM-treated *Rasa1*$^{fl/fl}$ *Ub*^{ert2cre} and *Rasa1*$^{fl/fl}$ *Cdh5*^{ert2cre} embryos, deletion efficiency of the *Rasa1* gene in BEC was comparable using the two different types of *ertcre* driver at E18.5 (Supplemental Figure 4). Therefore, differences in the time of onset of phenotypes cannot be explained by differences in *Rasa1* gene deletion

efficiency. In conclusion, disruption of *Rasa1* within EC during developmental angiogenesis is sufficient for the development of vascular abnormalities, including EC apoptosis, albeit that full manifestation of vascular phenotypes is slightly delayed.

Accumulation of collagen IV within BEC of induced EC-specific RASA1-deficient embryos. Since induced loss of RASA1 during developmental angiogenesis results in hemorrhage, we also examined the integrity of vascular BM. Vascular BM are composed predominantly of collagen IV and laminins that are produced mostly by EC but also VSMC during developmental angiogenesis (20). Apoptotic death of BEC would be expected to result in reduced deposition of BM that would result in reduced barrier function that could contribute to hemorrhage. To examine this, we stained skin sections from $Rasa1^{fl/fl}$ and $Rasa1^{fl/fl}\ Ub^{ert2cre}$ embryos that had been administered TM between E12.5 and E14.5 (or not) with antibodies against collagen IV (Supplemental Figures 1C and 5). As predicted, at E18.5-19.5, BV BM in TM-treated $Rasa1^{fl/fl}\ Ub^{ert2cre}$ embryos stained less intensely with collagen IV antibodies than BV BM in $Rasa1^{fl/fl}$ littermates (Supplemental Figure 5). In addition, in TM-treated $Rasa1^{fl/fl}\ Ub^{ert2cre}$ embryos, the collagen IV staining of BM was frequently discontinuous. Unexpected, however, was the finding that BEC in TM-treated $Rasa1^{fl/fl}\ Ub^{ert2cre}$ embryos frequently contained intracellular accumulations of collagen IV in discrete foci (Supplemental Figure 5). These abnormalities of collagen IV distribution were not observed in the absence of TM treatment (Supplemental Figure 1C).

To determine if intracellular collagen IV accumulation was a consequence of or was independent of BEC apoptosis, we stained skin sections of E18.5 *Rasa1*$^{fl/fl}$ *Cdh5*^{ert2cre} embryos administered TM at E13.5 with collagen IV antibodies (Figure 3). BEC apoptosis is observed infrequently in *Rasa1*$^{fl/fl}$ *Cdh5*^{ert2cre} embryos at this time point (Supplemental Figure 6). Nonetheless, BEC in these embryos (but not BEC in E18.5 *Rasa1*$^{fl/fl}$ *Cdh5*^{ert2cre} embryos that were not treated with TM) showed intracellular accumulation of collagen IV associated with a reduced density of collagen IV in BM (Figure 3 and Supplemental Figures 3 and 6). Therefore, intracellular accumulation of collagen IV occurs independently of BEC apoptosis. In contrast to collagen IV, laminin alpha 4 was deposited normally in BV BM in *Rasa1*$^{fl/fl}$ *Cdh5*^{ert2cre} embryos at E18.5 (Supplemental Figure 7). These findings indicate that impaired export of collagen IV from BEC is a contributing factor to the paucity of collagen IV in BV BM independent of BEC apoptosis. The intensity of collagen IV staining in BM of LV was also less in TM-treated E18.5 *Rasa1*$^{fl/fl}$ *Cdh5*^{ert2cre} embryos compared to controls (Supplemental Figure 8). Furthermore, this was associated with intracellular accumulation of collagen IV within LEC (Supplemental Figure 8). Therefore, similar to BV, intracellular accumulation of collagen IV in LEC likely contributes to the reduced density of collagen IV in LV BM following loss of RASA1.

Collagen IV is retained within the endoplasmic reticulum of EC of induced EC-specific RASA1-deficient embryos. Newly synthesized collagen IV in the endoplasmic reticulum (ER) is packaged into coat protein II (COPII)-coated vesicles that deliver collagen IV to the Golgi apparatus via the ER Golgi intermediate compartment (ERGIC). From the

Golgi, collagen IV is further packaged into secretory vesicles for export to the extracellular space (21). Potentially, therefore, intracellular accumulation of collagen IV in RASA1-deficient EC could be a result of retention in any of the ER, ERGIC or the Golgi itself. It is also theoretically possible that intracellular collagen IV reflects not impaired secretion but ingestion of collagen IV through an endocytic process. To examine this, skin sections from E18.5 *Rasa1*$^{fl/fl}$ *Cdh5*^{ert2cre} embryos treated with TM at E13.5 were co-stained with antibodies against collagen IV and organelle specific antibodies (Figure 4). No co-localization of collagen IV with ERGIC, Golgi or lysosomal markers was observed. In contrast, both of two different ER markers co-localized with collagen IV. Calnexin, a transmembrane ER chaperone, that is highly restricted to the ER, encircled discrete collagen IV punctae (22). In contrast, calreticulin, an ER lumenal chaperone was coincident with the majority of collagen IV punctae (Figure 4). Thus, intracellular collagen IV accumulation in RASA1-deficient EC is explained by impaired export of collagen IV from the ER.

Mechanism of EC death upon loss of RASA1 during developmental angiogenesis.
Blocked export of collagen IV from vascular cells could contribute to EC death during developmental angiogenesis in two distinct ways. First, blocked export could result in detachment or failed attachment of EC to vascular BM, thereby resulting in apoptotic death by anoikis (23). In this regard, we frequently observed EC with accumulated collagen IV in the process of detachment from the underlying BM following induced loss of RASA1 (Supplemental Figure 9). Furthermore, the notion that anoikis contributes to EC death in the absence of RASA1 is supported by the observation of an earlier EC

apoptotic response in TM-treated *Rasa1*$^{fl/fl}$ *Ub*^{ert2cre} compared to *Rasa1*$^{fl/fl}$ *Cdh5*^{ert2cre} embryos (Figures 1 and 2 and Table 1). Vascular BM collagen IV is synthesized both by EC and VSMC (20). In TM-treated *Rasa1*$^{fl/fl}$ *Ub*^{ert2cre} embryos, collagen IV export from both types of cell could be affected, resulting in less collagen IV deposition in BM compared to TM-treated *Rasa1*$^{fl/fl}$ *Cdh5*^{ert2cre} embryos in which export of collagen IV from EC only would be affected. To address this possibility, we examined if VSMC in *Rasa1*$^{fl/fl}$ *Ub*^{ert2cre} embryos also accumulated collagen IV following administration of TM. As predicted, intracellular accumulation of collagen IV was readily identified in VSMC cells of these embryos (Supplemental Figure 10). Furthermore, apoptotic VSMC were occasionally identified (Supplemental Figure 11).

A second mechanism through which accumulated intracellular collagen IV could induce EC apoptosis is through induction of ER stress resulting in an unfolded protein response (UPR) (24, 25). The purpose of the UPR is to assist the cell with the folding of unfolded and misfolded proteins in the ER. However, in circumstances where there remains an excess of unfolded protein, the UPR triggers apoptosis. In humans and mice, point-mutated collagen IV variants induce cell apoptosis via this mechanism (26-29). In addition, in mice deficient in the TANGO1 protein that is involved in export of collagen IV from the ER and in mice that are deficient in the Hsp47 chaperone that assists with collagen IV folding, accumulating wild-type collagen IV in the ER induces a UPR and BEC apoptosis (30, 31). The principal sensor of unfolded protein in the ER is BiP/Grp78, which is increased in expression during the course of a UPR. Therefore, to determine if a UPR is induced in BEC upon loss of RASA1 during developmental angiogenesis, we

examined expression of BiP. Amounts of BiP were sharply increased in EC of E18.5 *Rasa1*$^{fl/fl}$ *Cdh5*^{ert2cre} embryos treated with TM at E13.5 compared to EC in E18.5 *Rasa1*$^{fl/fl}$ controls and EC of E18.5 *Rasa1*$^{fl/fl}$ *Cdh5*^{ert2cre} embryos not treated with TM (Figure 5 and Supplemental Figure 12). These findings are consistent with the induction of a UPR in EC upon loss of RASA1.

The chemical chaperone 4-phenylbutyrate rescues blood vascular phenotypes in induced RASA1-deficient embryos. ER retention of collagen IV in RASA1-defcient BEC could be a direct consequence of impaired collagen IV folding in the ER or may instead be a result of altered expression or function of proteins involved in COPII-mediated protein secretion (32-34). To address this, we tested if a chemical chaperone, 4-phenylbutyrate (4PBA) could ameliorate vascular phenotypes that result from loss of RASA1. Previously it was demonstrated that 4PBA rescued blocked export of misfolded point mutant collagen IV variants from human and mouse EC in vitro and reversed intracerebral hemorrhage in mouse models that express these mutants (27, 35). Pregnant *Rasa1*$^{fl/fl}$ mice carrying *Rasa1*$^{fl/fl}$ and *Rasa1*$^{fl/fl}$ *Ub*^{ert2cre} embryos were administered TM with 4PBA at E13.5 followed by 4PBA every day thereafter until embryo harvest at E18.5. Administration of 4PBA in these experiments completely rescued each of EC export of collagen IV, EC apoptosis and blood vascular hemorrhage (Table 1 and Figure 6, compare Figure 1). In contrast, 4PBA had no influence upon vascular development when administered alone to embryos in the absence of TM (Supplemental Figure 13). As determined by real time qPCR of tail genomic DNA, 4PBA did not affect the ability of TM disrupt the *Rasa1* gene in *Rasa1*$^{fl/fl}$ *Ub*^{ert2cre} embryos (Supplemental Figure 14).

RASA1 siRNA-mediated knockdown of RASA1 in human umbilical vein endothelial cells (HUVEC) also resulted in intracellular accumulation of collagen IV, which could be rescued by 4PBA treatment (Figure 7). These findings provide strong evidence that blocked export of collagen IV from RASA1-deficient EC is a consequence of impaired collagen IV folding in the ER rather than a defect in COPII-mediated secretion.

Loss of RASA1 during developmental angiogenesis results in increased abundance of collagen IV-modifying enzymes in EC. Hetero-trimerization of two collagen IV alpha-1 monomers and one alpha-2 monomer and folding to form the mature protomer in the ER (collagen alpha-1 and alpha-2 are the predominant forms of collagen IV in EC) is a complex process that is regulated by different collagen IV-modifying enzymes and molecular chaperones that include protein disulfide isomerase A1 (PDIA1), peptidyl proline isomerases (PPIs), proline-4 and proline-3 hydroxylases (P4HA1-3 and P3H1-3 respectively), and lysine hydroxylases (LH1-3) also known as procollagen-lysine, 2-oxoglutarate 5-dioxygenase enzymes (PLOD1-3), and Hsp47. Potentially, therefore, increased or decreased abundance of collagen IV-modifying enzymes or chaperones in RASA1-deficient BEC impact upon collagen IV folding (36-40). To examine if loss of RASA1 resulted in changes in the amounts of collagen IV-modifying enzymes or chaperones in embryonic BEC during developmental angiogenesis, we performed proteomic analyses. Pregnant $Rasa1^{fl/fl}$ mice carrying $Rasa1^{fl/fl}$ and $Rasa1^{fl/fl}$ $Ub^{ert2cre}$ embryos were administered TM at E14.5 and embryos were harvested at E18.5, i.e. prior to BEC apoptosis and hemorrhage (Table 1). Subsequently, BEC were purified from skin of individual embryos, pooled according to genotype and lysed. Tryptic digests of lysates

were then analyzed by liquid chromatography-mass spectrometry/mass spectrometry (LC-MS/MS). With this approach we obtained data on the relative abundance of nearly 4,000 BEC proteins. Of these, approximately 250 proteins were increased at least 2-fold and 200 were decreased at least 2-fold in RASA1-deficient BEC compared to control BEC (Supplemental Table 1). Strikingly, several of the enzymes involved in collagen IV post-translational modification were increased in abundance, including FKBP9, P3H1, P4HA2, LH2/PLOD2, and LH3/PLOD3 (Table 2). In contrast, other ER resident proteins implicated in collagen folding, including PDIA1 and Hsp47, showed no or only modest changes in abundance. Furthermore, no significant changes in the abundance of any COPII secretory pathway proteins were apparent; consistent with the notion that impaired export of collagen IV is not a result of defects in the COPII secretion mechanism.

Inhibitors of 2-oxoglutarate (2OG) dependent oxygenases rescue blood vascular phenotypes in induced RASA1-deficient embryos. P4HA2, P3H1, PLOD2 and PLOD3 all belong to the same family of enzymes known as 2-oxoglutarate (2OG) dependent oxygenases, so called because of their dependency upon 2OG for catalysis (41). Consequently, drugs are available that generically inhibit all members of this family. One such drug is the catechol, ethyl-3,4-dihydroxybenzoic acid (EDHB) that has been used in vitro and in vivo to block the activity of collagen proline and lysine hydroxylases (41, 42). Therefore, to determine if increased abundance of any or all of these enzymes is responsible for collagen IV accumulation in BEC during developmental angiogenesis, we examined the ability of EDHB to rescue blocked collagen IV export and vascular phenotypes in induced RASA1-deficient embryos. Pregnant *Rasa1*$^{fl/fl}$ mice carrying

Rasa1$^{fl/fl}$ and *Rasa1*$^{fl/fl}$ *Ub*^{ert2cre} embryos were administered TM at E13.5 together with EDHB that was additionally administered to mice every day thereafter until embryo harvest at E18.5. Administration of EDHB in these experiments completely rescued EC export of collagen IV, EC apoptosis and blood vascular hemorrhage (Table 1 and Figure 8, compare Figure 1). In contrast, when administered to embryos in the absence of TM, EDHB did not affect vascular development (Supplemental Figure 15). As with 4PBA, EDHB did not affect *Rasa1* gene disruption induced by TM in *Rasa1*$^{fl/fl}$ *Ub*^{ert2cre} embryos (Supplemental Figure 14). The same results were obtained using another generic 2OG-dependent oxygenase inhibitor, 2,4 pyridinedicarboxylic acid (2,4PDCA) (Table 1, Supplemental Figure 14 and 16). These findings are consistent with a model in which loss of RASA1 in BEC during developmental angiogenesis results in increased amounts of collagen IV-modifying 2OG dependent oxygenases in BEC that accounts for collagen IV retention in the ER and downstream vascular phenotypes.

Dysregulated Ras-MAPK signaling is responsible for the development of BV phenotypes following RASA1 loss during developmental angiogenesis. RASA1 may participate in certain signaling pathways independently of its ability to regulate Ras (10). Therefore, to address if vascular phenotypes that result from induced loss of RASA1 during developmental angiogenesis result from dysregulated Ras signaling or to perturbation of a distinct signaling pathway, we examined *Rasa1*$^{fl/R780Q}$ *Ub*^{ert2cre} embryos that we have described previously (15, 17). Administration of TM to these embryos results in the expression of *Rasa1*^{R780Q} alone that encodes a catalytically inactive form of RASA1 in which all putative alternative functions of RASA1 are predicted to remain intact.

Pregnant *Rasa1*$^{fl/fl}$ mice carrying *Rasa1*$^{fl/fl}$ and *Rasa1*$^{fl/R780Q}$ embryos with and without *Ub*^{ert2cre} were administered TM at E12.5 and harvested at E18.5. Like *Rasa1*$^{fl/fl}$ *Ub*^{ert2cre} embryos (Figure 1), *Rasa1*$^{fl/R780Q}$ *Ub*^{ert2cre} embryos showed extensive hemorrhage and edema at E18.5 (Table 1 and Figure 9A). Furthermore, this was associated with accumulation of collagen IV in EC and EC apoptosis (Figure 9B). In contrast, the same vascular phenotypes were not apparent in E18.5 *Rasa1*$^{fl/+}$ *Ub*^{ert2cre} embryos induced to lose one *Rasa1* gene copy by administration of TM at E13.5 (Supplemental Figure 17). Thus, vascular phenotypes that result following loss of RASA1 during developmental angiogenesis are consequent to loss of an ability of RASA1 to regulate Ras and not loss of a Ras-independent function for this molecule.

Two well-characterized signaling pathways downstream of activated Ras are the MAPK and PI3K pathways. Potentially, therefore, augmented activation of either or both pathways could be responsible for BV phenotypes upon loss of RASA1 during developmental angiogenesis. To address this, *Rasa1*$^{fl/fl}$ mice carrying *Rasa1*$^{fl/fl}$ and *Rasa1*$^{fl/fl}$ *Ub*^{ert2cre} embryos were administered TM at E13.5 together with a MAPK pathway inhibitor (AZD6244) (43, 44) or a PI3K inhibitor (PX-866) (45) that were also administered to mice on the subsequent two days following the TM injection. As assessed at E18.5, the MAPK pathway inhibitor rescued the block in collagen IV export from BEC and prevented the development of hemorrhage in *Rasa1*$^{fl/fl}$ *Ub*^{ert2cre} embryos that is observed after TM treatment alone (Table 1 and Figure 10, compare Figure 1). AZD6244

did not affect TM-induced *Rasa1* gene deletion efficiency in *Rasa1*$^{fl/fl}$ *Ub*^{ert2cre} embryos (Supplemental Figure 14) and, by itself, AZD6244 did not induce any vascular abnormalities (Supplemental Figure 18). In contrast, the PI3K inhibitor was unable to rescue BEC export of collagen IV and apoptosis and extensive cutaneous hemorrhage was evident at E18.5 (data not shown). These findings show that dysregulated Ras-MAPK signaling rather than dysregulated Ras-PI3K signaling drives BV phenotypes upon RASA1 loss during developmental angiogenesis.

RASA1 is required for normal retinal angiogenesis in newborns. No spontaneous BV abnormalities have been noted in mice in which the *Rasa1* gene is disrupted after E15.5 (16, 17). We hypothesize that this is because the majority of the collagen IV in vascular BM is deposited during developmental angiogenesis. Collagen IV is recognized to be one of the most stable proteins in the animal kingdom (38). Thus, in postnatal life, continued high rate synthesis of collagen IV would be unnecessary in order for BEC to remain attached to BM. Nonetheless, in situations where de novo deposition of BM is required, abnormalities of BV function might be expected in RASA1-deficient mice. Two such situations are retinal angiogenesis in newborns and pathological angiogenesis in adults. To examine retinal angiogenesis, we administered TM to littermate *Rasa1*$^{fl/fl}$ *Ub*^{ert2cre} and *Rasa1*$^{fl/R780Q}$ *Ub*^{ert2cre} mice and cre-negative controls at P1 and examined the retinal vasculature at P4. The extent of new vessel growth in TM-treated *Rasa1*$^{fl/fl}$ *Ub*^{ert2cre} and *Rasa1*$^{fl/R780Q}$ *Ub*^{ert2cre} mice was significantly less than in *Rasa1*$^{fl/fl}$ controls as assessed by the number of vessel branch points and percentage coverage of the retina with BEC (Figure 11A,D). Furthermore, the number of BEC filopodia, which are a feature of

sprouting angiogenesis, at the periphery of the vascular coverage area, was reduced in the *Rasa1*$^{fl/fl}$ *Ub*^{ert2cre} and *Rasa1*$^{fl/R780Q}$ *Ub*^{ert2cre} mice (Figure 11B,D). Intracellular accumulation of collagen IV could be detected in retinal BEC of *Rasa1*$^{fl/fl}$ *Ub*^{ert2cre} and *Rasa1*$^{fl/R780Q}$ *Ub*^{ert2cre} mice but not *Rasa1*$^{fl/fl}$ control mice at P4 (Figure 11C). In addition, in *Rasa1*$^{fl/fl}$ *Ub*^{ert2cre} and *Rasa1*$^{fl/R780Q}$ *Ub*^{ert2cre} retinas, the number of "empty sleeves" that comprised of a thin tube of collagen IV with no BEC was substantially increased compared to controls (Figure 11C,D). This latter observation is consistent with impaired deposition of collagen IV into BM and BEC death during retinal angiogenesis in the absence of catalytically-active RASA1. Decreased angiogenesis was also observed in retinas of *Rasa1*$^{fl/fl}$ *Cdh5*^{ert2cre} mice administered TM at P1 and analyzed at P6 (Supplemental Figure 19), confirming an EC-intrinsic role for RASA1 in retinal angiogenesis. In *Rasa1*$^{fl/fl}$ *Ub*^{ert2cre} mice administered TM at P3, areas of hemorrhage were observed in retinas at P10 (Supplemental Figure 20).

Rasa1 is required for pathological angiogenesis in adults. To examine pathological angiogenesis, we initially used an ID8 ovarian tumor model (46). Adult littermate female *Rasa1*$^{fl/fl}$ and *Rasa1*$^{fl/fl}$ *Ub*^{ert2cre} mice were administered TM and 1 week later were injected in the flanks with ID8 tumor cells. Growth of injected ID8 tumor cells in female recipients is strictly dependent upon host BV angiogenesis. Six weeks after injection, ID8 tumors were substantially smaller in *Rasa1*$^{fl/fl}$ *Ub*^{ert2cre} mice compared to controls (Supplemental Figure 21A and B). Upon histological analysis, the density of BV in tumors from *Rasa1*$^{fl/fl}$ *Ub*^{ert2cre} mice was found to be substantially less than in tumors from control mice indicating that reduced tumor growth in the former was a result of

impaired BV tumor angiogenesis (Supplemental Figure 21C). Further analysis of BV in tumors of *Rasa1*$^{fl/fl}$ *Ub*^{ert2cre} mice revealed intracellular accumulation of collagen IV in BEC and BEC apoptosis (Supplemental Figure 21C and Supplemental Figure 22). Thus, blocked export of collagen IV from BEC and BEC apoptosis likely account for an impaired pathological angiogenesis response in the absence of RASA1.

To examine this further, we switched to a B16 melanoma model (47). B16 cells grow more rapidly than ID8 cells in vivo, thus permitting more ready analysis of the effect of drugs that promote collagen IV folding such as 4PBA. B16 were injected into the flanks of littermate TM-treated *Rasa1*$^{fl/fl}$ and *Rasa1*$^{fl/fl}$ *Ub*^{ert2cre} mice. Some mice were also injected with 4BPA at the same time that tumor cells were injected and additional 4PBA was administered to mice everyday thereafter. After 13 days, tumor growth and angiogenesis was assessed (Figure 12). As with ID8 tumor growth, B16 growth was inhibited in TM-treated *Rasa1*$^{fl/fl}$ *Ub*^{ert2cre} mice compared to *Rasa1*$^{fl/fl}$ controls (Figure 12A and B). In addition, the reduced growth of B16 tumors was also associated with impaired intra-tumoral BV angiogenesis and collagen IV accumulation in BEC (Figure 12C-E). 4PBA restored the growth of B16 cells in TM-treated *Rasa1*$^{fl/fl}$ *Ub*^{ert2cre} recipients and this was associated with normal export of collagen IV from BEC and BV angiogenesis (Figure 12). In contrast, 4PBA had no influence upon B16 growth in TM-treated *Rasa1*$^{fl/fl}$ mice (Figure 12) or when administered alone to *Rasa1*$^{fl/fl}$ and *Rasa1*$^{fl/fl}$ *Ub*^{ert2cre} mice that had not previously been injected with TM (Supplemental Figure 23). These findings are consistent with the notion that impaired pathological angiogenesis and

tumor growth in RASA1-deficient adult mice is also a consequence of an inability of BEC to export collagen IV for deposition in newly-forming basement membranes.

Discussion

In this study we show that RASA1 has a previously unappreciated critical function in the export of collagen IV from EC during developmental angiogenesis. In the absence of RASA1, collagen IV is retained in the ER of EC leading to their apoptotic death as a result of ER stress and anoikis. The chemical chaperone 4PBA rescues ER retention of collagen IV, EC apoptosis and BV hemorrhage in induced RASA1-deficient embryos. This finding strongly supports the notion that retention of collagen IV in the ER in the absence of RASA1 is a consequence of impaired protein folding. Further mechanistic studies indicated that loss of RASA1 within EC leads to dysregulated Ras-MAPK signaling that results in increased abundance of several ER-resident enzymes that carry out post-translational modifications of collagen IV that are known to regulate folding and ER export of this protein (36, 37). Most notable amongst these are P3H, P4H and PLOD enzymes of which there are three different isoforms each in mammals. Of the seven isoforms out of a total of nine that could be detected in BEC by LC-MS/MS, all were increased in abundance in RASA1-deficient BEC. Increased abundance of these enzymes could lead to excessive post-translation modification of collagen IV that would explain impaired folding and ER retention of this protein (36-40). Consistent with this, generic inhibitors of this class of enzymes, EDHB and 2,4PDCA, rescued ER collagen IV retention, EC apoptosis and hemorrhage in induced RASA1-deficient mice. This finding demonstrates that, although the abundance of numerous other proteins was also altered greater than 2-fold in RASA1 deficient BECs (Supplemental Table 1), increased abundance of these collagen IV modifying enzymes specifically is responsible for the development of vascular phenotypes in the absence of RASA1.

Dysregulated Ras-MAPK signaling could result in increased abundance of collagen IV-modifying enzymes as a result of increased gene transcription. MAPK modulate the activity of several different transcription factor complexes including activator protein 1 (AP1) complexes and ternary complex factors (TCFs) with the potential to modify transcription of collagen IV-modifying genes (48). Alternatively, dysregulated MAPK signaling could affect the abundance of these enzymes at a post-translational level, for example by phosphorylation of substrates that impact upon protein stability. To distinguish between these possibilities, we examined mRNA levels of two select enzymes, *Plod2* and *P3h1*, in sorted skin BEC from TM-treated *Rasa1*$^{fl/fl}$ and *Rasa1*$^{fl/fl}$ *Ub*^{ert2cre} embryos (Supplemental Figure 24). Levels of *Plod2* mRNA were significantly increased in *Rasa1*$^{fl/fl}$ *Ub*^{ert2cre} BEC consistent with increased *Plod2* transcription. In contrast, *P3h1* mRNA levels were not significantly increased in *Rasa1*$^{fl/fl}$ *Ub*^{ert2cre} BEC suggesting that loss of RASA1 in BEC results in increased abundance of P3H1 through a post-translational mechanism.

Whether impaired folding of collagen IV in RASA1-deficient EC is a result of a collective increase in the abundance of all three classes of collagen-modifying enzymes or to increased abundance of select enzymes remains to be determined. The collagenous domains of collagen IV contain multiple repeats of the sequence of Gly-Xaa-Yaa (where Xaa and Yaa are any amino acid). P4Hs hydroxylate prolines in the Yaa position whereas P3Hs subsequently hydroxylate prolines in the Xaa position of Gly-Xaa-4-hydroxyPro. PLODs hydroxylate lysine residues in the Yaa position of Gly-Xaa-Yaa and PLOD3

additionally catalyzes glycosylation of hydroxylysine to form galactosylhydroxylysine or galactosylglucosylhydroxylysine. Proline 3 hydroxylation is known to destabilize the collagen triple helix and, thus, excessive proline 3 hydroxylation of collagen IV is likely an important contributor to impaired folding (38-40). In contrast, proline 4 hydroxylation promotes electrostatic interactions between collagen IV monomers and lysine hydroxylation and glycosylation is required for collagen IV secretion (36-38). Nonetheless, increased abundance of P4Hs and PLODs could lead to excessive modification that could also negatively impact upon folding of collagen protomers.

Vasculogenesis commonly results in the formation of a vascular plexus that comprises of a primitive vascular network with presumptive arterial inputs and venous outputs. Subsequently, angiogenic processes that include fusion, intussusception, regression and sprouting angiogenesis remodel the plexus to yield a hierarchical network of arteries, arterioles, venules and veins connected by smaller diameter capillaries (18). Previous studies of global EPHB4-deficient and RASA1-deficient mice have provided evidence that AVMs and AFs in CM-AVM arise as a consequence of impaired angiogenic remodeling of these primitive vascular plexuses (49). Thus, in EPHB4-deficient embryos and in embryos of mice deficient in the EPHB4 ligand, Ephrin B2, arteries form near direct connections with veins through large diameter vessels, as observed in CM-AVM (50, 51). Similarly, in RASA1-deficient embryos, the same defect in angiogenic remodeling of vascular plexuses has also been noted (14). In these regards, findings in this study are directly relevant to an understanding of the pathogenesis of CM-AVM. Potentially, acquisition of somatic second hit mutations in *RASA1* in EC or their

precursors at the time of or prior to vasculogenesis respectively could result in the loss of RASA1 in the majority of EC in an individual primitive vessel within a vascular plexus. Consequently, sprouting angiogenesis and potentially other forms of angiogenesis from that vessel would be blocked as these events would require de novo synthesis of collagen IV by EC in these vessels and deposition of collagen IV in newly forming BM. Thus, an inability of EC in these vessels to export collagen IV during angiogenic remodeling could potentially account for the development of AVM and AF in CM-AVM. Alternatively, acquisition of second hit mutations in *RASA1* in EC later in development, after remodeling of vascular plexuses, could result in CM, again as a consequence of blocked export of collagen IV. In either scenario, the ability of chemical chaperones and inhibitors of 2OG dependent oxygenases to rescue impaired developmental angiogenesis in the absence of RASA1 suggests possible means of prevention of vascular lesions in human embryos and patients with inherited *RASA1* mutations. Whether such drugs would be effective in the treatment of existing vascular lesions in CM-AVM is far less certain. EC of CM-AVM lesions would not be expected to be engaged in high rate synthesis of collagen IV and, in the absence of angiogenic stimuli, intracellular accumulation of collagen IV in EC of lesions would not be predicted nor would it be expected to contribute to lesion pathology. To confirm this, we examined collagen IV accumulation in CM and AVM lesions of multiple CM-AVM1 patients, including two patients in which somatic inactivating second hit *RASA1* mutations had been identified in lesional tissue. Intracellular collagen IV accumulation was not apparent in EC of theses lesions, again, as predicted (Supplemental Figure 25).

Lymphatic vessel abnormalities have also been reported in CM-AVM and may also be explained by impaired angiogenic remodeling of primitive lymphatic vascular plexuses as a consequence of LEC retention of collagen IV (2-7). In addition, RASA1 is required for the development of LV valves (17). Therefore, second hit mutations of *RASA1*, if they were to affect a sufficient number of valve-forming LEC at a site of valvulogenesis, could impact upon leaflet development in that vessel that would contribute to lymphatic dysfunction. Formation of LV valves requires coordinated LEC synthesis and deposition of extracellular matrix proteins, including collagen IV, into a leaflet extracellular matrix core to which LEC attach (52, 53). Therefore, an inability of valve-forming LEC to export collagen IV for deposition in this matrix core would provide a logical explanation for failed LV valve development. Furthermore, this would be consistent with the observation that in the absence of RASA1, LEC in valve-forming regions initially up-regulate expression of PROX1 that is a characteristic of valve-forming LEC but then undergo apoptosis resulting in failed valve development (17).

The absence of spontaneous BV abnormalities following loss of RASA1 in mice at any point after birth is consistent with a model in which continued high rate synthesis of collagen IV by BEC is not necessary for BV function. Exceptions to this would include retinal angiogenesis in newborns and pathological angiogenesis in adults where EC synthesis of collagen IV and deposition in BM would be necessary. Accordingly, we show here that RASA1 is required for both processes and, at least for pathological angiogenesis, evidence indicates that impaired angiogenesis is again consequent to an inability of EC to export collagen IV. Earlier studies of pathological angiogenesis and

retinal angiogenesis in mice indicated that miR-132-mediated down regulation of *Rasa1* mRNA in EC is required in order for Ras activation and for angiogenesis to proceed (54, 55). The current studies do not contradict this notion but instead explore the consequences of complete and permanent loss of RASA1 in EC. miR-132-mediated down-regulation of *Rasa1* during normal angiogenesis is likely not complete and would be expected to be transient. In contrast, genetic disruption of *Rasa1* would result in chronic uncontrolled activation of Ras in EC with distinct downstream consequences. In this regard, it is of note that mice that express constitutively-active H-Ras (resistant to RasGAP-mediated inactivation) in EC develop brain vascular malformations and hemorrhagic stroke (56). Moreover, somatic activating mutations in K-Ras have been identified in the majority of brain AVMs in humans (57). The effect of induced loss of RASA1 upon retinal angiogenesis and pathological angiogenesis induced by actively growing tumors had not previously been examined. The current studies, therefore, are the first to address this question.

Notably, RASA1 is also required for the maintenance of LEC number in LV valves in adults. We propose that the loss of LEC in adult valves upon RASA1 loss reflects a requirement for valve leaflet LEC to engage in high rate collagen IV synthesis in order to remain attached to leaflets that encounter higher shear stress forces than LV or BV wall EC (52, 53). Indeed, shear stress has been shown to induce collagen IV expression in EC beforehand (58). Whether RASA1 is also required for the maintenance of BECs in venous valves that would encounter similarly high sheer stress forces remains to be determined.

Methods

For a full description of Methods, see Supplemental Methods online.

Mice. *Rasa1*$^{fl/fl}$ and *Rasa1*$^{fl/R780Q}$ mice with and without *Ub*^{ert2cre} transgenes have been described (15-17, 59). *Cdh5*^{ert2cre} mice were obtained from Cancer Research UK (London, UK). *Rasa1*$^{fl/fl}$ *Cdh5*^{ert2cre} mice were generated through cross-breeding. All mice were on a mixed 129S6/SvEv X C57BL/6 genetic background.

Statistics. Statistical analysis was performed using Student's 1-sample and 2-sample t tests or one-way ANOVA tests with a Dunnett's multiple comparisons post-hoc test as indicated. A *P* value less than 0.05 was considered significant.

Study approval. All experiments performed with mice were in compliance with University of Michigan guidelines and were approved by the university committee on the use and care of animals. All work performed with CM-AVM1 tissue samples was approved by the Institutional Review Boards at the respective institutions.

Author contributions

DC, PEL and PDK contributed to the design of studies. DC performed the majority of experiments with assistance from PEL. JT and PN provided CM-AVM1 tissue samples. PN assisted with interpretation of findings. The manuscript was written by PDK.

Acknowledgements

This work was supported by NIH grant HL120888 to PDK. Project consultation and mass spectrometry data analysis was performed at the Proteomics & Peptide Synthesis Core of the University of Michigan by Dr. Henriette A Remmer. The experimental processing was contracted with MS Bioworks LLC.

References

1. Eerola I, Boon LM, Mulliken JB, Burrows PE, Dompmartin A, Watanabe S, Vanwijck R, and Vikkula M. Capillary malformation-arteriovenous malformation, a new clinical and genetic disorder caused by RASA1 mutations. *Am J Hum Genet.* 2003;73(6):1240-9.
2. Revencu N, Boon LM, Mendola A, Cordisco MR, Dubois J, Clapuyt P, Hammer F, Amor DJ, Irvine AD, Baselga E, et al. RASA1 mutations and associated phenotypes in 68 families with capillary malformation-arteriovenous malformation. *Hum Mutat.* 2013;34(12):1632-41.
3. Revencu N, Boon LM, Mulliken JB, Enjolras O, Cordisco MR, Burrows PE, Clapuyt P, Hammer F, Dubois J, Baselga E, et al. Parkes Weber syndrome, vein of Galen aneurysmal malformation, and other fast-flow vascular anomalies are caused by RASA1 mutations. *Hum Mutat.* 2008;29(7):959-65.
4. Burrows PE, Gonzalez-Garay ML, Rasmussen JC, Aldrich MB, Guilliod R, Maus EA, Fife CE, Kwon S, Lapinski PE, King PD, et al. Lymphatic abnormalities are associated with RASA1 gene mutations in mouse and man. *Proc Natl Acad Sci U S A.* 2013.
5. de Wijn RS, Oduber CE, Breugem CC, Alders M, Hennekam RC, and van der Horst CM. Phenotypic variability in a family with capillary malformations caused by a mutation in the RASA1 gene. *Eur J Med Genet.* 2012;55(3):191-5.
6. Macmurdo CF, Wooderchak-Donahue W, Bayrak-Toydemir P, Le J, Wallenstein MB, Milla C, Teng JM, Bernstein JA, and Stevenson DA. RASA1 somatic

mutation and variable expressivity in capillary malformation/arteriovenous malformation (CM/AVM) syndrome. *Am J Med Genet A.* 2016;170(6):1450-4.

7. Sevick-Muraca EM, and King PD. Lymphatic vessel abnormalities arising from disorders of Ras signal transduction. *Trends Cardiovasc Med.* 2014;24(3):121-7.

8. Buday L, and Downward J. Many faces of Ras activation. *Biochim Biophys Acta.* 2008;1786(2):178-87.

9. Wennerberg K, Rossman KL, and Der CJ. The Ras superfamily at a glance. *J Cell Sci.* 2005;118(Pt 5):843-6.

10. King PD, Lubeck BA, and Lapinski PE. Nonredundant functions for Ras GTPase-activating proteins in tissue homeostasis. *Sci Signal.* 2013;6(264):re1.

11. Lapinski PE, Doosti A, Salato V, North P, Burrows PE, and King PD. Somatic second hit mutation of RASA1 in vascular endothelial cells in capillary malformation-arteriovenous malformation. *Eur J Med Genet.* 2018;61(1):11-6.

12. Amyere M, Revencu N, Helaers R, Pairet E, Baselga E, Cordisco M, Chung W, Dubois J, Lacour JP, Martorell L, et al. Germline Loss-of-Function Mutations in EPHB4 Cause a Second Form of Capillary Malformation-Arteriovenous Malformation (CM-AVM2) Deregulating RAS-MAPK Signaling. *Circulation.* 2017;136(11):1037-48.

13. Kawasaki J, Aegerter S, Fevurly RD, Mammoto A, Mammoto T, Sahin M, Mably JD, Fishman SJ, and Chan J. RASA1 functions in EPHB4 signaling pathway to suppress endothelial mTORC1 activity. *J Clin Invest.* 2014;124(6):2774-84.

14. Henkemeyer M, Rossi DJ, Holmyard DP, Puri MC, Mbamalu G, Harpal K, Shih TS, Jacks T, and Pawson T. Vascular system defects and neuronal apoptosis in mice lacking ras GTPase-activating protein. *Nature.* 1995;377(6551):695-701.

15. Lubeck BA, Lapinski PE, Bauler TJ, Oliver JA, Hughes ED, Saunders TL, and King PD. Blood vascular abnormalities in Rasa1(R780Q) knockin mice: implications for the pathogenesis of capillary malformation-arteriovenous malformation. *Am J Pathol.* 2014;184(12):3163-9.

16. Lapinski PE, Kwon S, Lubeck BA, Wilkinson JE, Srinivasan RS, Sevick-Muraca E, and King PD. RASA1 maintains the lymphatic vasculature in a quiescent functional state in mice. *J Clin Invest.* 2012;122(2):733-47.

17. Lapinski PE, Lubeck BA, Chen D, Doosti A, Zawieja SD, Davis MJ, and King PD. RASA1 regulates the function of lymphatic vessel valves in mice. *J Clin Invest.* 2017;127(7):2569-85.

18. Udan RS, Culver JC, and Dickinson ME. Understanding vascular development. *Wiley Interdiscip Rev Dev Biol.* 2013;2(3):327-46.

19. Wang Y, Nakayama M, Pitulescu ME, Schmidt TS, Bochenek ML, Sakakibara A, Adams S, Davy A, Deutsch U, Luthi U, et al. Ephrin-B2 controls VEGF-induced angiogenesis and lymphangiogenesis. *Nature.* 2010;465(7297):483-6.

20. Glentis A, Gurchenkov V, and Matic Vignjevic D. Assembly, heterogeneity, and breaching of the basement membranes. *Cell Adh Migr.* 2014;8(3):236-45.

21. Malhotra V, and Erlmann P. The pathway of collagen secretion. *Annu Rev Cell Dev Biol.* 2015;31(109-24.

22. Butler J, Watson HR, Lee AG, Schuppe HJ, and East JM. Retrieval from the ER-golgi intermediate compartment is key to the targeting of c-terminally anchored ER-resident proteins. *J Cell Biochem.* 2011;112(12):3543-8.

23. Michel JB. Anoikis in the cardiovascular system: known and unknown extracellular mediators. *Arterioscler Thromb Vasc Biol.* 2003;23(12):2146-54.

24. Kim I, Xu W, and Reed JC. Cell death and endoplasmic reticulum stress: disease relevance and therapeutic opportunities. *Nat Rev Drug Discov.* 2008;7(12):1013-30.

25. Oslowski CM, and Urano F. The binary switch between life and death of endoplasmic reticulum-stressed beta cells. *Curr Opin Endocrinol Diabetes Obes.* 2010;17(2):107-12.

26. Guiraud S, Migeon T, Ferry A, Chen Z, Ouchelouche S, Verpont MC, Sado Y, Allamand V, Ronco P, and Plaisier E. HANAC Col4a1 Mutation in Mice Leads to Skeletal Muscle Alterations due to a Primary Vascular Defect. *Am J Pathol.* 2017;187(3):505-16.

27. Jeanne M, Jorgensen J, and Gould DB. Molecular and Genetic Analyses of Collagen Type IV Mutant Mouse Models of Spontaneous Intracerebral Hemorrhage Identify Mechanisms for Stroke Prevention. *Circulation.* 2015;131(18):1555-65.

28. Jeanne M, Labelle-Dumais C, Jorgensen J, Kauffman WB, Mancini GM, Favor J, Valant V, Greenberg SM, Rosand J, and Gould DB. COL4A2 mutations impair COL4A1 and COL4A2 secretion and cause hemorrhagic stroke. *Am J Hum Genet.* 2012;90(1):91-101.

29. Weng YC, Sonni A, Labelle-Dumais C, de Leau M, Kauffman WB, Jeanne M, Biffi A, Greenberg SM, Rosand J, and Gould DB. COL4A1 mutations in patients with sporadic late-onset intracerebral hemorrhage. *Ann Neurol.* 2012;71(4):470-7.

30. Marutani T, Yamamoto A, Nagai N, Kubota H, and Nagata K. Accumulation of type IV collagen in dilated ER leads to apoptosis in Hsp47-knockout mouse embryos via induction of CHOP. *J Cell Sci.* 2004;117(Pt 24):5913-22.

31. Wilson DG, Phamluong K, Li L, Sun M, Cao TC, Liu PS, Modrusan Z, Sandoval WN, Rangell L, Carano RA, et al. Global defects in collagen secretion in a Mia3/TANGO1 knockout mouse. *J Cell Biol.* 2011;193(5):935-51.

32. Saito K, and Katada T. Mechanisms for exporting large-sized cargoes from the endoplasmic reticulum. *Cell Mol Life Sci.* 2015;72(19):3709-20.

33. Unlu G, Levic DS, Melville DB, and Knapik EW. Trafficking mechanisms of extracellular matrix macromolecules: insights from vertebrate development and human diseases. *Int J Biochem Cell Biol.* 2014;47(57-67.

34. Melville DB, Montero-Balaguer M, Levic DS, Bradley K, Smith JR, Hatzopoulos AK, and Knapik EW. The feelgood mutation in zebrafish dysregulates COPII-dependent secretion of select extracellular matrix proteins in skeletal morphogenesis. *Dis Model Mech.* 2011;4(6):763-76.

35. Kuo DS, Labelle-Dumais C, Mao M, Jeanne M, Kauffman WB, Allen J, Favor J, and Gould DB. Allelic heterogeneity contributes to variability in ocular dysgenesis, myopathy and brain malformations caused by Col4a1 and Col4a2 mutations. *Hum Mol Genet.* 2014;23(7):1709-22.

36. Chioran A, Duncan S, Catalano A, Brown TJ, and Ringuette MJ. Collagen IV trafficking: The inside-out and beyond story. *Dev Biol.* 2017;431(2):124-33.

37. Ishikawa Y, and Bachinger HP. A molecular ensemble in the rER for procollagen maturation. *Biochim Biophys Acta.* 2013;1833(11):2479-91.

38. Shoulders MD, and Raines RT. Collagen structure and stability. *Annu Rev Biochem.* 2009;78(929-58.

39. Mizuno K, Hayashi T, Peyton DH, and Bachinger HP. The peptides acetyl-(Gly-3(S)Hyp-4(R)Hyp)10-NH2 and acetyl-(Gly-Pro-3(S)Hyp)10-NH2 do not form a collagen triple helix. *J Biol Chem.* 2004;279(1):282-7.

40. Jenkins CL, Bretscher LE, Guzei IA, and Raines RT. Effect of 3-hydroxyproline residues on collagen stability. *J Am Chem Soc.* 2003;125(21):6422-7.

41. Rose NR, McDonough MA, King ON, Kawamura A, and Schofield CJ. Inhibition of 2-oxoglutarate dependent oxygenases. *Chem Soc Rev.* 2011;40(8):4364-97.

42. Gilkes DM, Chaturvedi P, Bajpai S, Wong CC, Wei H, Pitcairn S, Hubbi ME, Wirtz D, and Semenza GL. Collagen prolyl hydroxylases are essential for breast cancer metastasis. *Cancer Res.* 2013;73(11):3285-96.

43. Engelman JA, Chen L, Tan X, Crosby K, Guimaraes AR, Upadhyay R, Maira M, McNamara K, Perera SA, Song Y, et al. Effective use of PI3K and MEK inhibitors to treat mutant Kras G12D and PIK3CA H1047R murine lung cancers. *Nat Med.* 2008;14(12):1351-6.

44. Pratilas CA, and Solit DB. Targeting the mitogen-activated protein kinase pathway: physiological feedback and drug response. *Clin Cancer Res.* 2010;16(13):3329-34.

45. Courtney KD, Corcoran RB, and Engelman JA. The PI3K pathway as drug target in human cancer. *J Clin Oncol.* 2010;28(6):1075-83.

46. Su F, Kozak KR, Imaizumi S, Gao F, Amneus MW, Grijalva V, Ng C, Wagner A, Hough G, Farias-Eisner G, et al. Apolipoprotein A-I (apoA-I) and apoA-I mimetic peptides inhibit tumor development in a mouse model of ovarian cancer. *Proc Natl Acad Sci U S A.* 2010;107(46):19997-20002.

47. Jablonska J, Leschner S, Westphal K, Lienenklaus S, and Weiss S. Neutrophils responsive to endogenous IFN-beta regulate tumor angiogenesis and growth in a mouse tumor model. *J Clin Invest.* 2010;120(4):1151-64.

48. Chang L, and Karin M. Mammalian MAP kinase signalling cascades. *Nature.* 2001;410(6824):37-40.

49. Fish JE, and Wythe JD. The molecular regulation of arteriovenous specification and maintenance. *Dev Dyn.* 2015;244(3):391-409.

50. Adams RH, Wilkinson GA, Weiss C, Diella F, Gale NW, Deutsch U, Risau W, and Klein R. Roles of ephrinB ligands and EphB receptors in cardiovascular development: demarcation of arterial/venous domains, vascular morphogenesis, and sprouting angiogenesis. *Genes Dev.* 1999;13(3):295-306.

51. Gerety SS, Wang HU, Chen ZF, and Anderson DJ. Symmetrical mutant phenotypes of the receptor EphB4 and its specific transmembrane ligand ephrin-B2 in cardiovascular development. *Mol Cell.* 1999;4(3):403-14.

52. Bazigou E, and Makinen T. Flow control in our vessels: vascular valves make sure there is no way back. *Cell Mol Life Sci.* 2013;70(6):1055-66.

53. Bazigou E, Wilson JT, and Moore JE, Jr. Primary and secondary lymphatic valve development: molecular, functional and mechanical insights. *Microvasc Res.* 2014;96(38-45.

54. Anand S, Majeti BK, Acevedo LM, Murphy EA, Mukthavaram R, Scheppke L, Huang M, Shields DJ, Lindquist JN, Lapinski PE, et al. MicroRNA-132-mediated loss of p120RasGAP activates the endothelium to facilitate pathological angiogenesis. *Nat Med.* 2010;16(8):909-14.

55. Westenskow PD, Kurihara T, Aguilar E, Scheppke EL, Moreno SK, Wittgrove C, Marchetti V, Michael IP, Anand S, Nagy A, et al. Ras pathway inhibition prevents neovascularization by repressing endothelial cell sprouting. *J Clin Invest.* 2013;123(11):4900-8.

56. Li QF, Decker-Rockefeller B, Bajaj A, and Pumiglia K. Activation of Ras in the Vascular Endothelium Induces Brain Vascular Malformations and Hemorrhagic Stroke. *Cell Rep.* 2018;24(11):2869-82.

57. Nikolaev SI, Vetiska S, Bonilla X, Boudreau E, Jauhiainen S, Rezai Jahromi B, Khyzha N, DiStefano PV, Suutarinen S, Kiehl TR, et al. Somatic Activating KRAS Mutations in Arteriovenous Malformations of the Brain. *N Engl J Med.* 2018;378(3):250-61.

58. Yamane T, Mitsumata M, Yamaguchi N, Nakazawa T, Mochizuki K, Kondo T, Kawasaki T, Murata S, Yoshida Y, and Katoh R. Laminar high shear stress up-regulates type IV collagen synthesis and down-regulates MMP-2 secretion in endothelium. A quantitative analysis. *Cell Tissue Res.* 2010;340(3):471-9.

59. Lapinski PE, Bauler TJ, Brown EJ, Hughes ED, Saunders TL, and King PD. Generation of mice with a conditional allele of the p120 Ras GTPase-activating protein. *Genesis*. 2007;45(12):762-7.

Table 1. Embryonic disruption of *Rasa1*

Littermate group	*Rasa1*	*Ert2Cre* driver	TM day	Drug[a]	Harvest	Embryonic vascular phenotypes	Percentage embryos with phenotype (affected/total)
1	*fl/fl*	*Ub*	E12.5	None	E18.5	Hemorrhage/lymphedema EC apoptosis[c]	100 (11/11)
	fl/fl	None	E12.5	None	E18.5	None	0 (0/5)
2	*fl/fl*	*Ub*	E13.5	None	E18.5	Hemorrhage/lymphedema EC apoptosis[c]	91 (10/11)
	fl/fl	None	E13.5	None	E18.5	None	0 (0/8)
3	*fl/fl*	*Ub*	E13.5	4PBA[a]	E18.5	None	0 (0/7)
	fl/fl	None	E13.5	4PBA[a]	E18.5	None	0 (0/5)
4	*fl/fl*	*Ub*	E13.5	EDHB[a]	E18.5	None	0 (0/5)
	fl/fl	None	E13.5	EDHB[a]	E18.5	None	0 (0/7)
5	*fl/fl*	*Ub*	E13.5	2,4PDCA[a]	E18.5	None	0 (0/3)
	fl/fl	None	E13.5	2,4PDCA[a]	E18.5	None	0 (0/6)
6	*fl/fl*	*Ub*	E13.5	AZD6244[b]	E18.5	None	0 (0/7)
	fl/fl	None	E13.5	AZD6244[a]	E18.5	None	0 (0/8)
7	*fl/fl*	*Ub*	E14.5	None	E19.5	Hemorrhage/lymphedema EC apoptosis[c]	100 (1/1)
	fl/fl	None	E14.5	None	E19.5	None	0 (0/2)
8	*fl/fl*	*Ub*	E15.5	None	E17.5	Valve LEC apoptosis Impaired lymphatic vessel valve development[c]	100 (6/6) Ref. 17
	fl/fl	None	E15.5	None	E17.5	None	Ref. 17
9	*fl/fl*	*Cdh5*	E13.5	None	E18.5	Hemorrhage (local)[c]	83 (10/12)
	fl/fl	None	E13.5	None	E18.5	None	0 (0/6)
10	*fl/fl*	*Cdh5*	E13.5	None	E19.5	Hemorrhage/lymphedema EC apoptosis[c]	100 (7/7)
	fl/fl	None	E13.5	None	E19.5	None	0 (0/5)
11	*fl/R780Q*	*Ub*	E12.5	None	E18.5	Hemorrhage/lymphedema EC apoptosis[c]	86 (6/7)
	fl/R780Q	None	E12.5	None	E18.5	None	0 (0/6)

[a] Administered at same time as TM and everyday thereafter until E18.5
[b] Administered at same time as TM and on following 2 days
[c] Phenotypes not apparent prior to this time

Table 2. Abundance of collagen IV modifying enzymes in RASA1-deficient embryonic BEC[a]		
Protein	**Function**	**Cre+/Cre-**
PDIA1	PDI	1.4
PPIB	PPI (ER)	0.8
FKBP2	PPI (ER)	0.8
FKBP7	PPI (ER)	0.7
FKBP9[b]	PPI (ER)	2.1
FKBP10	PPI (ER)	1.2
P3H1	P3H	2.1
P3H3	P3H	>5[c]
P4HA1	P4H	1.7
P4HA2	P4H	3.4
PLOD1	PLOD	1.6
PLOD2	PLOD	5.1
PLOD3	PLOD	2
HSP47	HSP	1.2

[a]Abundance of all detectable known collagen IV-modifying enzymes and chaperones are shown

[b]Proteins with 2-fold or greater changes in abundance are indicated with grey shading

[c]P3H3 was undetectable in control cells and thus fold increase is of uncertain significance

Figure legends

Figure 1. Hemorrhage, edema and EC apoptosis following global disruption of *Rasa1* during developmental angiogenesis. (**A**) TM was administered to littermate *Rasa1*$^{fl/fl}$ and *Rasa1*$^{fl/fl}$ *Ub*^{ert2cre} embryos at E13.5 and embryos were harvested at E18.5. *Rasa1*$^{fl/fl}$ *Ub*^{ert2cre} embryos show extensive cutaneous hemorrhage that was confirmed by staining of skin sections with H&E. Sections were additionally stained with antibodies against CD31 and LYVE-1 to identify BV and LV respectively. Note abundant BV and LV in skin of control *Rasa1*$^{fl/fl}$ embryos (separate representative fields are shown) and damaged BV and absence of LV in skin of *Rasa1*$^{fl/fl}$ *Ub*^{ert2cre} embryos (separate fields show areas with and without extravasated auto-fluorescent erythrocytes in yellow). (**B**) TM was administered to littermate *Rasa1*$^{fl/fl}$ and *Rasa1*$^{fl/fl}$ *Ub*^{ert2cre} embryos at E12.5 and embryos were harvested at E18.5. Skin sections were stained with Hoechst and antibodies against CD31 and activated caspase 3. Note activated caspase 3 (arrows) surrounding fragmented nuclei of apoptotic BEC of *Rasa1*$^{fl/fl}$ *Ub*^{ert2cre} embryos. (**C**) Quantitation of BEC apoptosis in skin BV of *Rasa1*$^{fl/fl}$ and *Rasa1*$^{fl/fl}$ *Ub*^{ert2cre} embryos administered TM at E12.5 and harvested at E18.5. Shown is the mean +/- 1 SEM of the percentage of activated caspase 3+ BEC per BV (n=10 BV each genotype). ****, $P<0.0001$, Student's 2-sample t-test.

Figure 2. BV abnormalities following disruption of *Rasa1* specifically within EC during developmental angiogenesis. TM was administered to littermate *Rasa1*$^{fl/fl}$ and *Rasa1*$^{fl/fl}$ *Cdh5*^{ert2cre} embryos at E13.5. (**A** and **B**) Embryos were harvested at E18.5 or E19.5 and skin sections were stained with H&E. Note localized hemorrhage in *Rasa1*$^{fl/fl}$

Cdh5^{ert2cre} embryos at E18.5 (arrows) and more extensive hemorrhage and edema at E19.5. Note extravasated erythrocytes in skin sections from E18.5 and E19.5 embryos. The section from the E18.5 *Rasa1*$^{fl/fl}$ *Cdh5*^{ert2cre} embryo is from an area of skin with visible hemorrhage. (**C**) Embryos were harvested at E19.5 and skin sections were stained with Hoechst and antibodies against CD31 and activated caspase 3. Note apoptotic BEC in *Rasa1*$^{fl/fl}$ *Cdh5*^{ert2cre} embryos (arrows).

Figure 3. EC-specific disruption of *Rasa1* during developmental angiogenesis results in retention of collagen IV within BEC. TM was administered to littermate *Rasa1*$^{fl/fl}$ and *Rasa1*$^{fl/fl}$ *Cdh5*^{ert2cre} embryos at E13.5. Embryos were harvested at E18.5 and skin sections were stained with Hoechst and antibodies against CD31 and collagen IV. Lower power images are shown in top rows. Higher power images of boxed areas are shown below, Note accumulation of collagen IV within BEC of *Rasa1*$^{fl/fl}$ *Cdh5*^{ert2cre} embryos (arrows).

Figure 4. Collagen IV is trapped within the ER of BEC following disruption of *Rasa1* during developmental angiogenesis. Skin sections from E18.5 *Rasa1*$^{fl/fl}$ *Cdh5*^{ert2cre} embryos administered TM at E13.5 were stained with Hoechst and antibodies against collagen IV together with antibodies against calnexin (ER), calreticulin (ER), LMNA1 (ERGIC), TGN46 (Golgi) or LAMP-1 (lysosome). Note encircling of collagen IV punctae with calnexin (arrows) and colocalization with calreticulin (arrows) but absence of colocalization of collagen IV punctae with other organelle markers (arrowheads). N, nucleus; E, erythrocyte.

Figure 5. Increased amounts of BIP in BEC following disruption of *Rasa1* during developmental angiogenesis. Skin sections from E18.5 *Rasa1*$^{fl/fl}$ *Cdh5*^{ert2cre} embryos administered TM at E13.5 were stained with Hoechst and antibodies against CD31 and BIP. Note increased BIP in BEC of the *Rasa1*$^{fl/fl}$ *Cdh5*^{ert2cre} embryos indicative of an ongoing UPR (arrows).

Figure 6. Rescue of developmental angiogenesis defects in induced RASA1-deficient mice with the chemical chaperone 4PBA. TM was administered to littermate *Rasa1*$^{fl/fl}$ and *Rasa1*$^{fl/fl}$ *Ub*^{ert2cre} embryos at E13.5. 4PBA was co-administered with the TM and was also administered to embryos on consecutive days thereafter until embryo harvest at E18.5. (**A**) Gross appearance of embryos. Note absence of hemorrhage and edema in *Rasa1*$^{fl/fl}$ *Ub*^{ert2cre} embryos that was confirmed by H&E staining of skin sections. (**B**) Skin sections were stained with Hoechst and antibodies against collagen IV, CD31 and activated caspase 3. Note normal deposition of collagen IV in vascular BM and absence of BEC apoptosis in *Rasa1*$^{fl/fl}$ *Ub*^{ert2cre} embryos.

Figure 7. RASA1 knockdown in HUVEC results in collagen IV accumulation in the ER that can be rescued by 4PBA. HUVEC were transfected with control or *RASA1* siRNA and cultured for 24 hours in the presence or absence of 4PBA. (**A**) Cells were stained with Hoechst and antibodies against collagen IV and calnexin. Representative images are shown. Note intracellular accumulation of collagen IV in *RASA1* siRNA-treated cells and its rescue by 4PBA treatment. (**B**) Higher magnification images of

RASA1 siRNA-treated cells in (A) to show large intracellular accumulations of collagen IV surrounded by calnexin. (**C**) Knockdown of *RASA1* was confirmed by reverse transcriptase qPCR. Shown is the mean +/- 1 SEM of the amount of *RASA1* mRNA normalized to the *RASA1* mRNA level in control siRNA-treated HUVEC in the same experiment (n=2). (**D**) Mean +/- 1 SEM of the percentage of HUVEC per field with evidence of intracellular collagen IV accumulation (n=12). *, $P<0.05$, ****, $P<0.0001$, ns, not significant, one-way ANOVA test with a Dunnett's multiple comparisons post-hoc test.

Figure 8. Rescue of developmental angiogenesis defects in induced RASA1-deficient mice with the 2OG dependent oxygenase inhibitor, EDHB. TM was administered to littermate $Rasa1^{fl/fl}$ and $Rasa1^{fl/fl}$ $Ub^{ert2cre}$ embryos at E13.5. EDHB was co-administered with the TM and was also administered to embryos on consecutive days thereafter until embryo harvest at E18.5. (**A**) Gross appearance of embryos. Note absence of hemorrhage and edema in $Rasa1^{fl/fl}$ $Ub^{ert2cre}$ embryos that was confirmed by H&E staining of skin sections. (**B**) Skin sections were stained with Hoechst and antibodies against collagen IV, CD31 and activated caspase 3. Note normal deposition of collagen IV in vascular BM and absence of BEC apoptosis in $Rasa1^{fl/fl}$ $Ub^{ert2cre}$ embryos.

Figure 9. BV abnormalities in embryos induced to express RASA1 R780Q alone during developmental angiogenesis. TM was administered to littermate $Rasa1^{fl/R780Q}$ and $Rasa1^{fl/R780Q}$ $Ub^{ert2cre}$ embryos at E12.5 and embryos were harvested at E18.5. (**A**)

Gross appearance of embryos. Note cutaneous hemorrhage in *Rasa1*$^{fl/R780Q}$ *Ub*^{ert2cre} embryos confirmed by H&E staining of skin sections. (**B**) Skin sections were stained with Hoechst and antibodies against collagen IV, CD31 and activated caspase 3. Note discontinuous distribution of collagen IV in BV BM, accumulation of collagen IV in BEC and presence of activated caspase 3 in nuclei of BEC (arrows) of *Rasa1*$^{fl/R780Q}$ *Ub*^{ert2cre} embryos. (**C**) Quantitation of BEC apoptosis in skin BV of *Rasa1*$^{fl/R780Q}$ and *Rasa1*$^{fl/R780}$ *Ub*^{ert2cre} embryos administered TM at E12.5 and harvested at E18.5. Shown is the mean +/- 1 SEM of the percentage of activated caspase 3+ BEC per BV (n=15 BV each genotype). ****, $P<0.0001$, Student's 2-sample t-test.

Figure 10. An inhibitor of MAPK signaling blocks the development of BV abnormalities resulting from induced loss of RASA1 during developmental angiogenesis. TM was administered to littermate *Rasa1*$^{fl/fl}$ and *Rasa1*$^{fl/fl}$ *Ub*^{ert2cre} embryos at E13.5. The MAPK pathway inhibitor, AZD6244, was co-administered with the TM and was also administered to embryos on the following two days afterward. Embryos were harvested at E18.5. (**A**) Gross appearance of embryos. Note absence of hemorrhage and edema in *Rasa1*$^{fl/fl}$ *Ub*^{ert2cre} embryos that was confirmed by H&E staining of skin sections. (**B**) Skin sections were stained with Hoechst and antibodies against collagen IV and CD31. Note normal deposition of collagen IV in vascular BM in *Rasa1*$^{fl/fl}$ *Ub*^{ert2cre} embryos.

Figure 11. Impaired retinal angiogenesis in neonatal induced RASA1 R780Q and RASA1-deficient mice. TM was administered to littermate *Rasa1*$^{fl/fl}$, *Rasa1*$^{fl/R780Q}$*Ub*^{ert2cre} and *Rasa1*$^{fl/fl}$ *Ub*^{ert2cre} mice at P1 and retinas were harvested at P4. (**A-C**) Retinas were stained with isolectin B4 (IB4) to identify BV and anti-collagen IV (**C**). (**A,B**) Representative low (**A**) and high (**B**) power images of IB4 staining are shown. *, filopodia at the vascular front. (**C**) High power images (left) to show collagen IV accumulation in BEC of *Rasa1*$^{fl/R780Q}$*Ub*^{ert2cre} and *Rasa1*$^{fl/fl}$ *Ub*^{ert2cre} retinas (arrows) and lower power images (right) to illustrate empty collagen IV sleeves in *Rasa1*$^{fl/R780Q}$*Ub*^{ert2cre} and *Rasa1*$^{fl/fl}$ *Ub*^{ert2cre} retinas (arrows). (**D**) Graphs show mean +/- 1 SEM of the number of branch points from veins (n=6 retinas each genotype), the percentage coverage of retinas with BEC per field (n=5-7 retinas each genotype), the number of filopodia per vascular field (n=7-10 retinas each genotype), and the number of empty collagen sleeves per field (n=5-8 retinas each genotype). **, $P<0.01$; ***, $P<0.001$,****, $P<0.0001$, one-way ANOVA test with a Dunnett's multiple comparisons post-hoc test.

Figure 12. Disruption of *Rasa1* in adult mice inhibits pathological angiogenesis in a B16 melanoma model. Littermate adult *Rasa1*$^{fl/fl}$ and *Rasa1*$^{fl/fl}$ *Ub*^{ert2cre} mice were administered TM before subcutaneous injection of B16 melanoma cells into flanks one week later. 4PBA was administered to some mice at the same time as B16 melanoma cells and every day thereafter for the duration of the experiment. After 13 days, mice were euthanized and tumors were harvested. (**A**) Representative images of harvested tumors are shown. (**B**) Graphs show mean +/- 1 SEM of tumor weight and volume (n=5-8 tumors from mice of each genotype and treatment condition). (**C**) Sections of tumors

were stained with Hoechst and CD31 antibodies. Representative images show reduced BV density in tumors from *Rasa1*$^{fl/fl}$ *Ub*^{ert2cre} mice treated TM alone. (**D**) Graph shows mean +/- 1 SEM of percentage coverage of fields with BV (n=5-6 tumors from mice of each genotype and treatment condition). (**E**) Tumor sections were stained with Hoechst and antibodies against collagen IV and CD31. Representative images are shown. Note accumulation of collagen IV in BEC of tumors from *Rasa1*$^{fl/fl}$ *Ub*^{ert2cre} mice treated with TM alone (arrows). *, $P<0.05$, **, $P<0.01$; ns, not significant, one-way ANOVA test with a Dunnett's multiple comparisons post-hoc test.

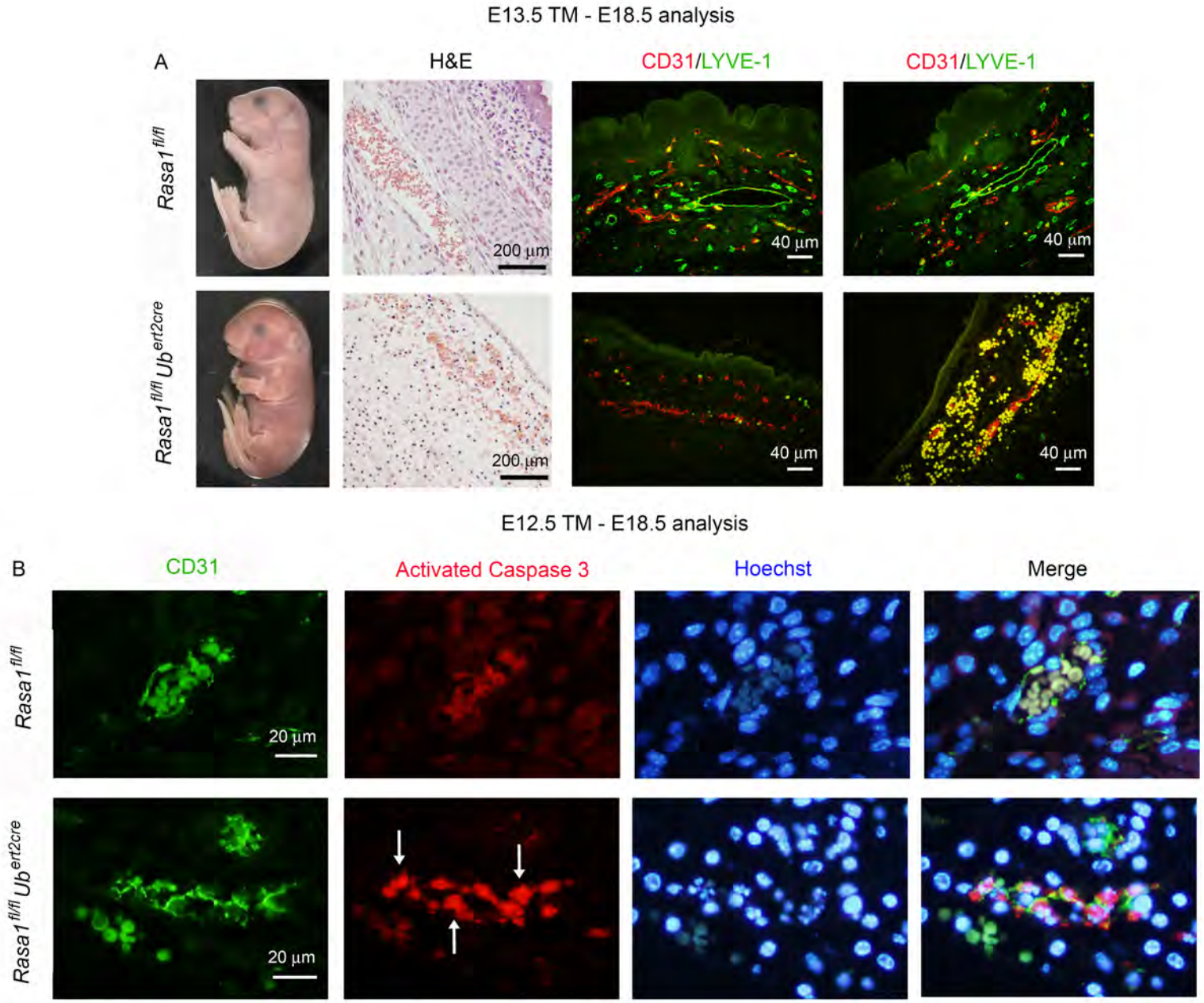

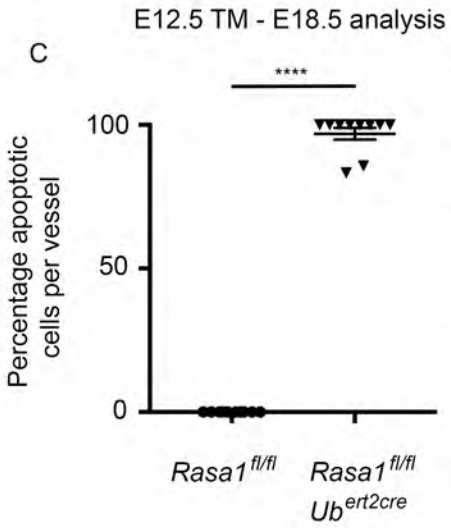

Figure 1. Hemorrhage, edema and EC apoptosis following global disruption of *Rasa1* during developmental angiogenesis. (**A**) TM was administered to littermate *Rasa1*$^{fl/fl}$ and *Rasa1*$^{fl/fl}$ *Ub*^{ert2cre} embryos at E13.5 and embryos were harvested at E18.5. *Rasa1*$^{fl/fl}$ *Ub*^{ert2cre} embryos show extensive cutaneous hemorrhage that was confirmed by staining of skin sections with H&E. Sections were additionally stained with antibodies against CD31 and LYVE-1 to identify BV and LV respectively. Note abundant BV and LV in skin of control *Rasa1*$^{fl/fl}$ embryos (separate representative fields are shown) and damaged BV and absence of LV in skin of *Rasa1*$^{fl/fl}$ *Ub*^{ert2cre} embryos (separate fields show areas with and without extravasated auto-fluorescent erythrocytes in yellow). (**B**) TM was administered to littermate *Rasa1*$^{fl/fl}$ and *Rasa1*$^{fl/fl}$ *Ub*^{ert2cre} embryos at E12.5 and embryos were harvested at E18.5. Skin sections were stained with Hoechst and antibodies against CD31 and activated caspase 3. Note activated caspase 3 (arrows) surrounding fragmented nuclei of apoptotic BEC of *Rasa1*$^{fl/fl}$ *Ub*^{ert2cre} embryos. (**C**) Quantitation of BEC apoptosis in skin BV of *Rasa1*$^{fl/fl}$ and *Rasa1*$^{fl/fl}$ *Ub*^{ert2cre} embryos administered TM at E12.5 and harvested at E18.5. Shown is the mean +/- 1 SEM of the percentage of activated caspase 3+ BEC per BV (n=10 BV each genotype). ****, $P<0.0001$, Student's 2-sample t-test.

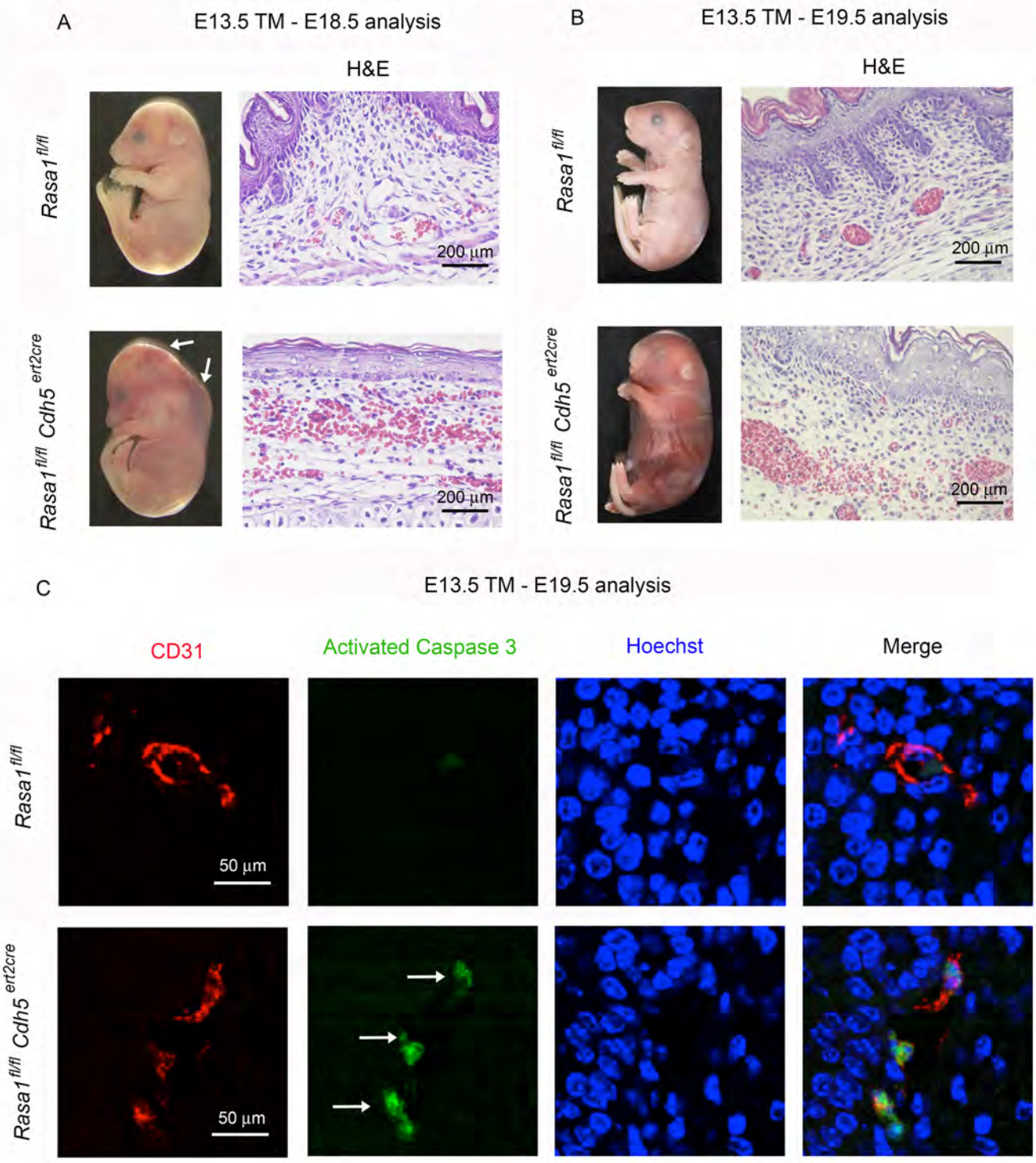

Figure 2. BV abnormalities following disruption of *Rasa1* specifically within EC during developmental angiogenesis. TM was administered to littermate *Rasa1*$^{fl/fl}$ and *Rasa1*$^{fl/fl}$ *Cdh5*^{ert2cre} embryos at E13.5. (**A** and **B**) Embryos were harvested at E18.5 or E19.5 and skin sections were stained with H&E. Note localized hemorrhage in *Rasa1*$^{fl/fl}$ *Cdh5*^{ert2cre} embryos at E18.5 (arrows) and more extensive hemorrhage and edema at E19.5. Note extravasated erythrocytes in skin sections from E18.5 and E19.5 embryos. The section from the E18.5 *Rasa1*$^{fl/fl}$ *Cdh5*^{ert2cre} embryo is from an area of skin with visible hemorrhage. (**C**) Embryos were harvested at E19.5 and skin sections were stained with Hoechst and antibodies against CD31 and activated caspase 3. Note apoptotic BEC in *Rasa1*$^{fl/fl}$ *Cdh5*^{ert2cre} embryos (arrows).

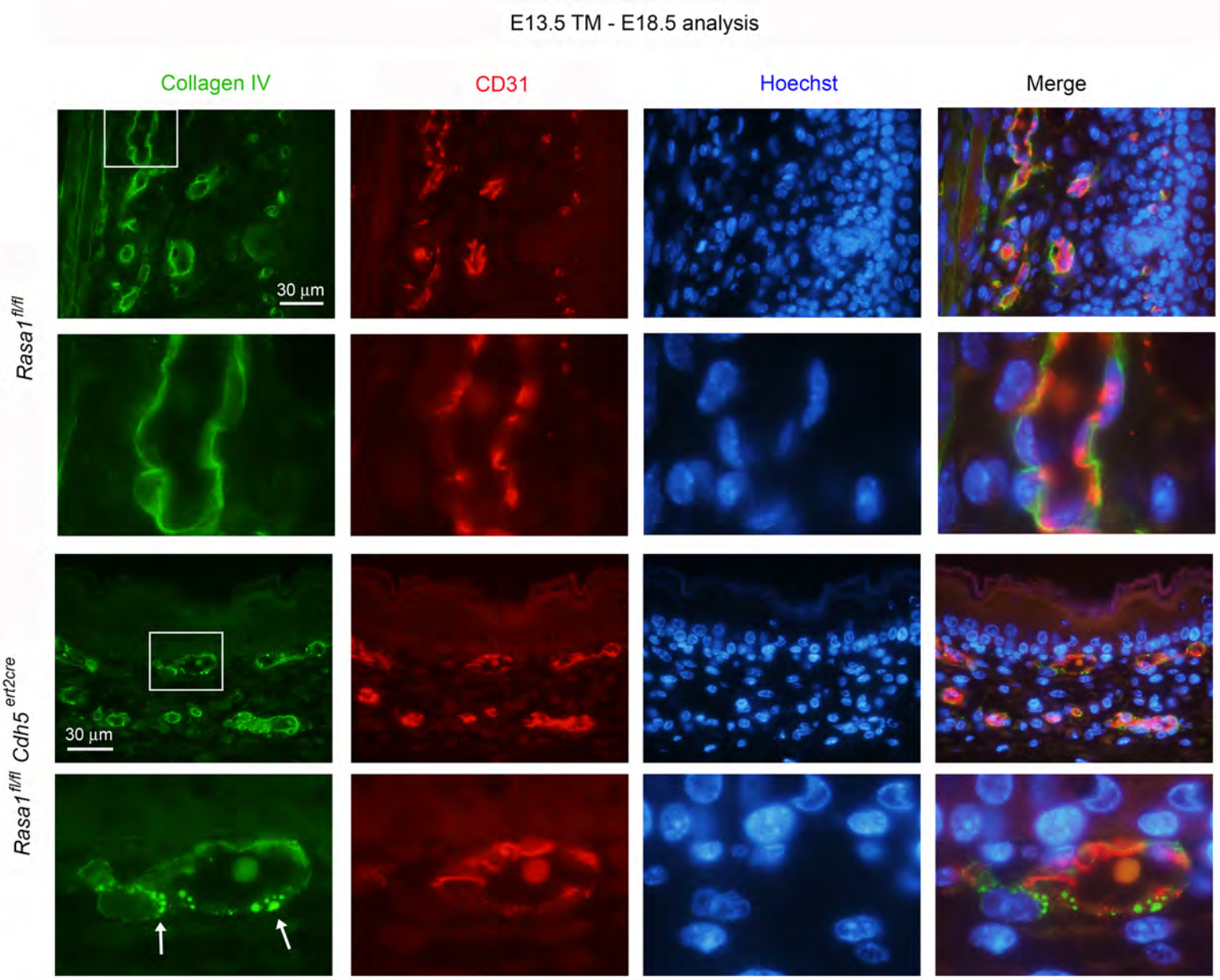

Figure 3. EC-specific disruption of *Rasa1* during developmental angiogenesis results in retention of collagen IV within BEC. TM was administered to littermate *Rasa1*$^{fl/fl}$ and *Rasa1*$^{fl/fl}$ *Cdh5*^{ert2cre} embryos at E13.5. Embryos were harvested at E18.5 and skin sections were stained with Hoechst and antibodies against CD31 and collagen IV. Lower power images are shown in top rows. Higher power images of boxed areas are shown below, Note accumulation of collagen IV within BEC of *Rasa1*$^{fl/fl}$ *Cdh5*^{ert2cre} embryos (arrows).

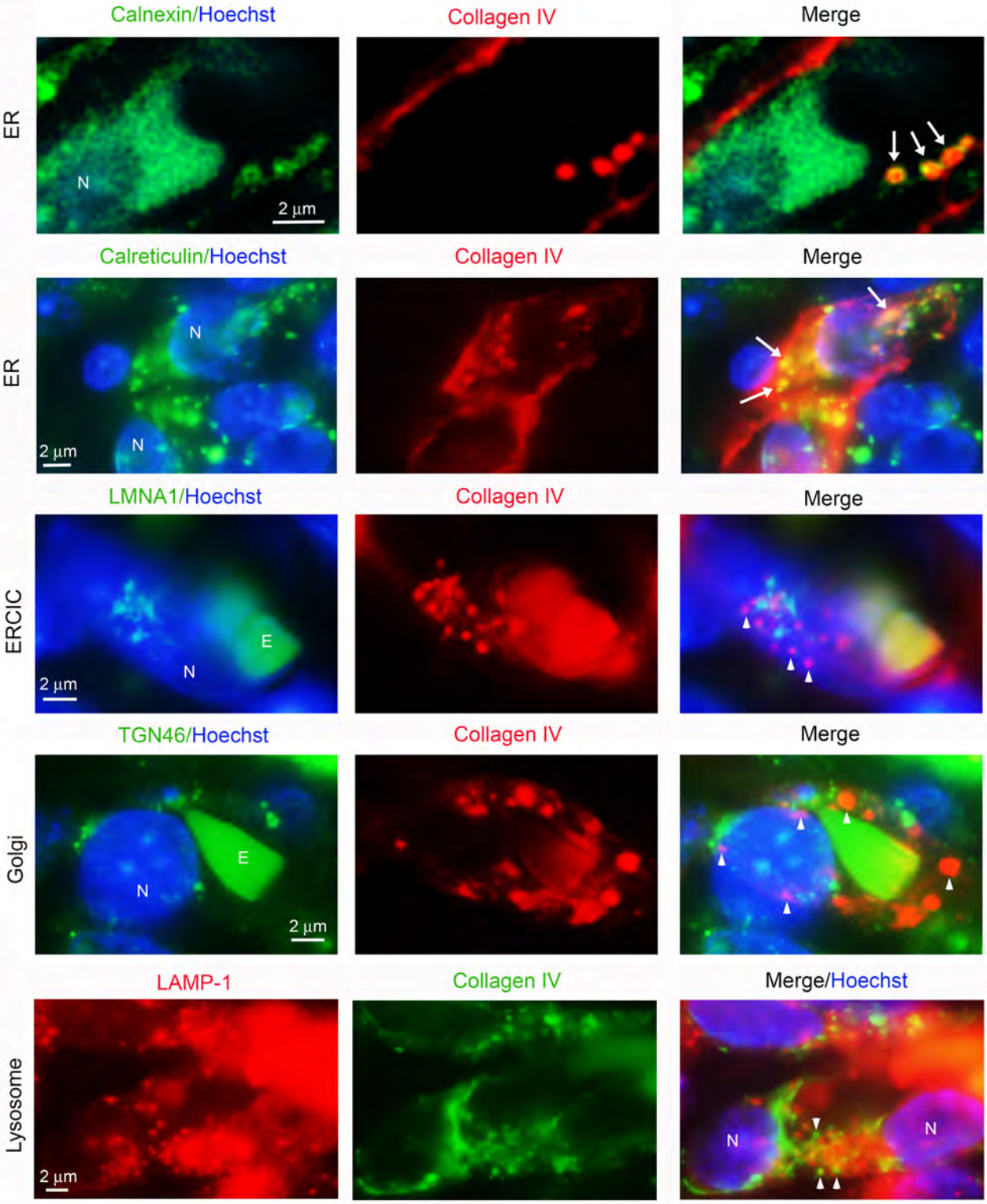

Figure 4. Collagen IV is trapped within the ER of BEC following disruption of *Rasa1* during developmental angiogenesis. Skin sections from E18.5 *Rasa1*$^{fl/fl}$ *Cdh5*^{ert2cre} embryos administered TM at E13.5 were stained with Hoechst and antibodies against collagen IV together with antibodies against calnexin (ER), calreticulin (ER), LMNA1 (ERGIC), TGN46 (Golgi) or LAMP-1 (lysosome). Note encircling of collagen IV punctae with calnexin (arrows) and colocalization with calreticulin (arrows) but absence of colocalization of collagen IV punctae with other organelle markers (arrowheads). N, nucleus; E, erythrocyte.

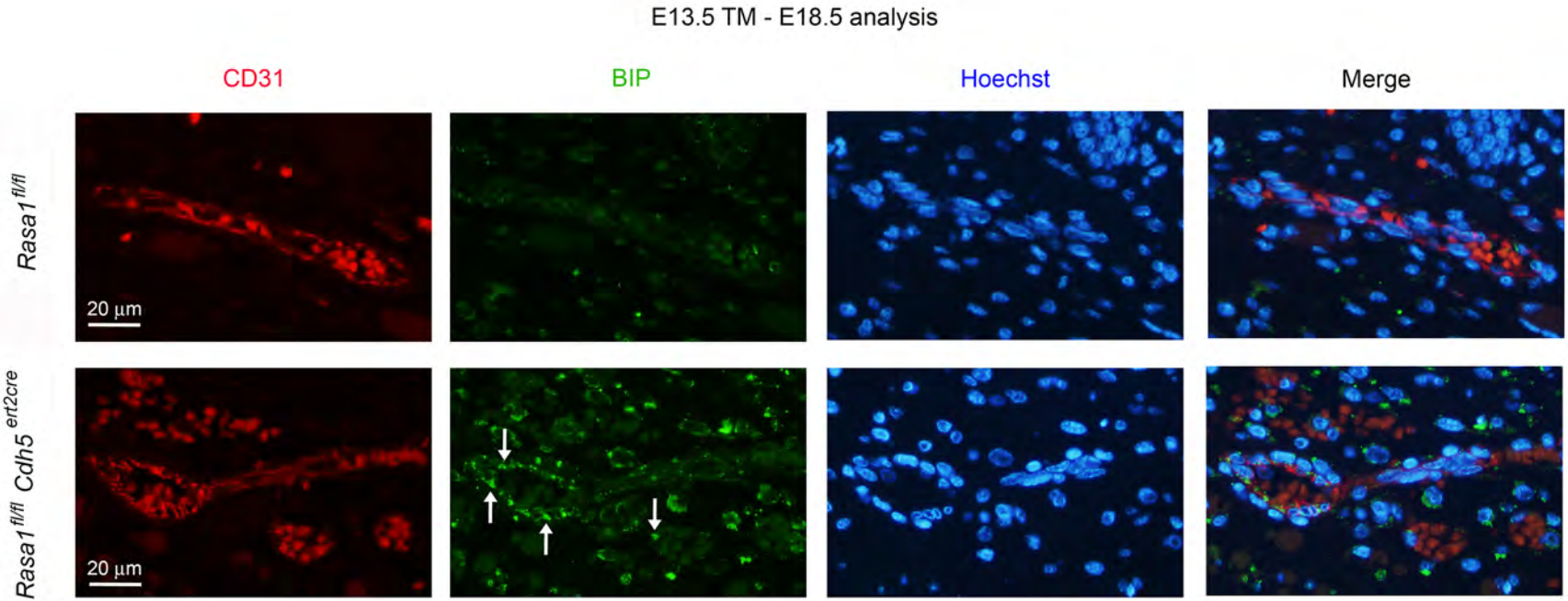

Figure 5. Increased amounts of BIP in BEC following disruption of *Rasa1* during developmental angiogenesis. Skin sections from E18.5 *Rasa1*$^{fl/fl}$ *Cdh5*^{ert2cre} embryos administered TM at E13.5 were stained with Hoechst and antibodies against CD31 and BIP. Note increased BIP in BEC of the *Rasa1*$^{fl/fl}$ *Cdh5*^{ert2cre} embryos indicative of an ongoing UPR (arrows).

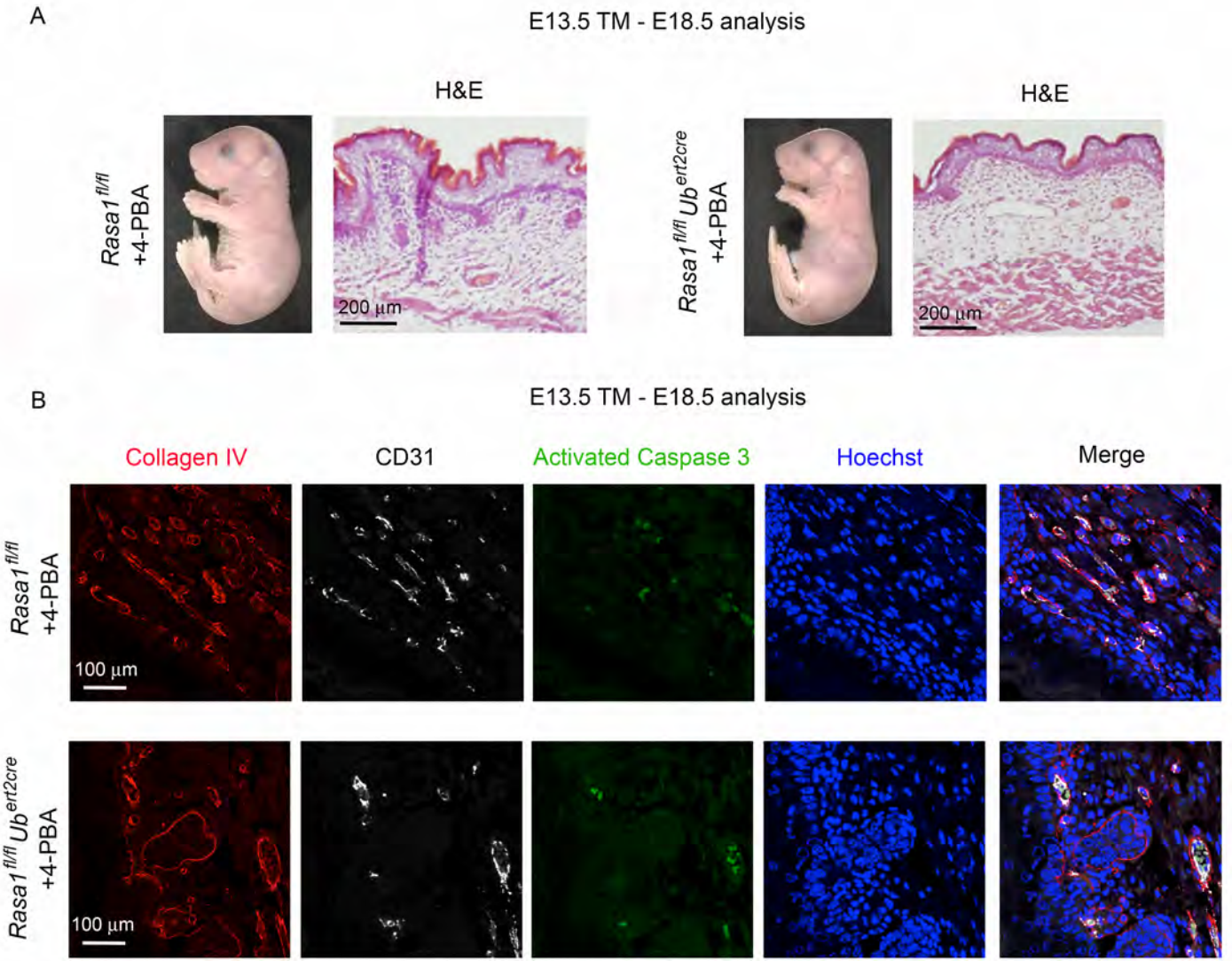

Figure 6. Rescue of developmental angiogenesis defects in induced RASA1-deficient mice with the chemical chaperone 4PBA. TM was administered to littermate *Rasa1*$^{fl/fl}$ and *Rasa1*$^{fl/fl}$ *Ub*^{ert2cre} embryos at E13.5. 4PBA was co-administered with the TM and was also administered to embryos on consecutive days thereafter until embryo harvest at E18.5. (**A**) Gross appearance of embryos. Note absence of hemorrhage and edema in *Rasa1*$^{fl/fl}$ *Ub*^{ert2cre} embryos that was confirmed by H&E staining of skin sections. (**B**) Skin sections were stained with Hoechst and antibodies against collagen IV, CD31 and activated caspase 3. Note normal deposition of collagen IV in vascular BM and absence of BEC apoptosis in *Rasa1*$^{fl/fl}$ *Ub*^{ert2cre} embryos.

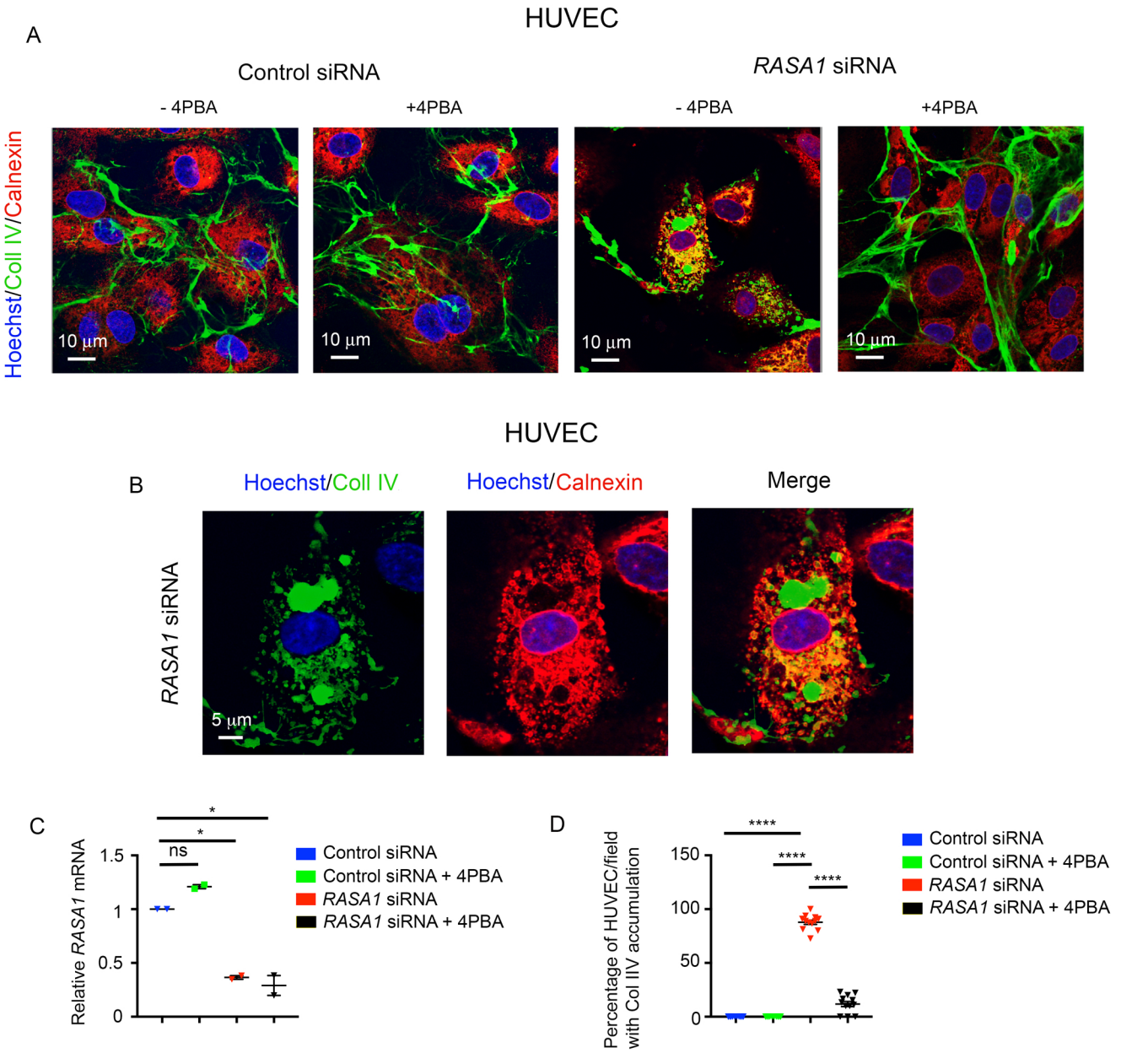

Figure 7. RASA1 knockdown in HUVEC results in collagen IV accumulation in the ER that can be rescued by 4PBA. HUVEC were transfected with control or *RASA1* siRNA and cultured for 24 hours in the presence or absence of 4PBA. (**A**) Cells were stained with Hoechst and antibodies against collagen IV and calnexin. Representative images are shown. Note intracellular accumulation of collagen IV in *RASA1* siRNA-treated cells and its rescue by 4PBA treatment. (**B**) Higher magnification images of *RASA1* siRNA-treated cells in (A) to show large intracellular accumulations of collagen IV surrounded by calnexin. (**C**) Knockdown of *RASA1* was confirmed by reverse transcriptase qPCR. Shown is the mean +/- 1 SEM of the amount of *RASA1* mRNA normalized to the *RASA1* mRNA level in control siRNA-treated HUVEC in the same experiment (n=2). (**D**) Mean +/- 1 SEM of the percentage of HUVEC per field with evidence of intracellular collagen IV accumulation (n=12). *, $P<0.05$, ****, $P<0.0001$, ns, not significant, one-way ANOVA test with a Dunnett's multiple comparisons post-hoc test.

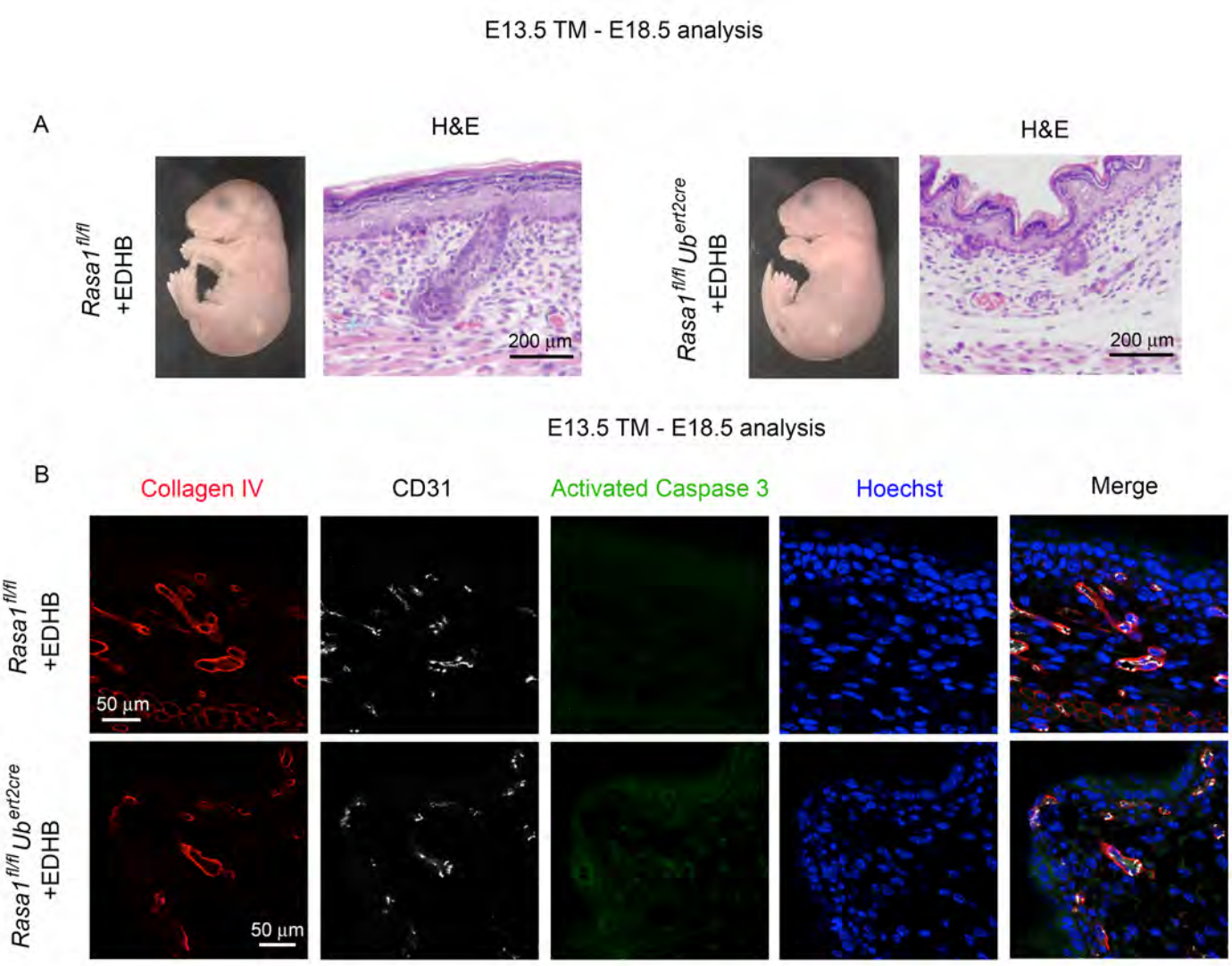

Figure 8. Rescue of developmental angiogenesis defects in induced RASA1-deficient mice with the 2OG dependent oxygenase inhibitor, EDHB. TM was administered to littermate *Rasa1*$^{fl/fl}$ and *Rasa1*$^{fl/fl}$ *Ub*^{ert2cre} embryos at E13.5. EDHB was co-administered with the TM and was also administered to embryos on consecutive days thereafter until embryo harvest at E18.5. (**A**) Gross appearance of embryos. Note absence of hemorrhage and edema in *Rasa1*$^{fl/fl}$ *Ub*^{ert2cre} embryos that was confirmed by H&E staining of skin sections. (**B**) Skin sections were stained with Hoechst and antibodies against collagen IV, CD31 and activated caspase 3. Note normal deposition of collagen IV in vascular BM and absence of BEC apoptosis in *Rasa1*$^{fl/fl}$ *Ub*^{ert2cre} embryos.

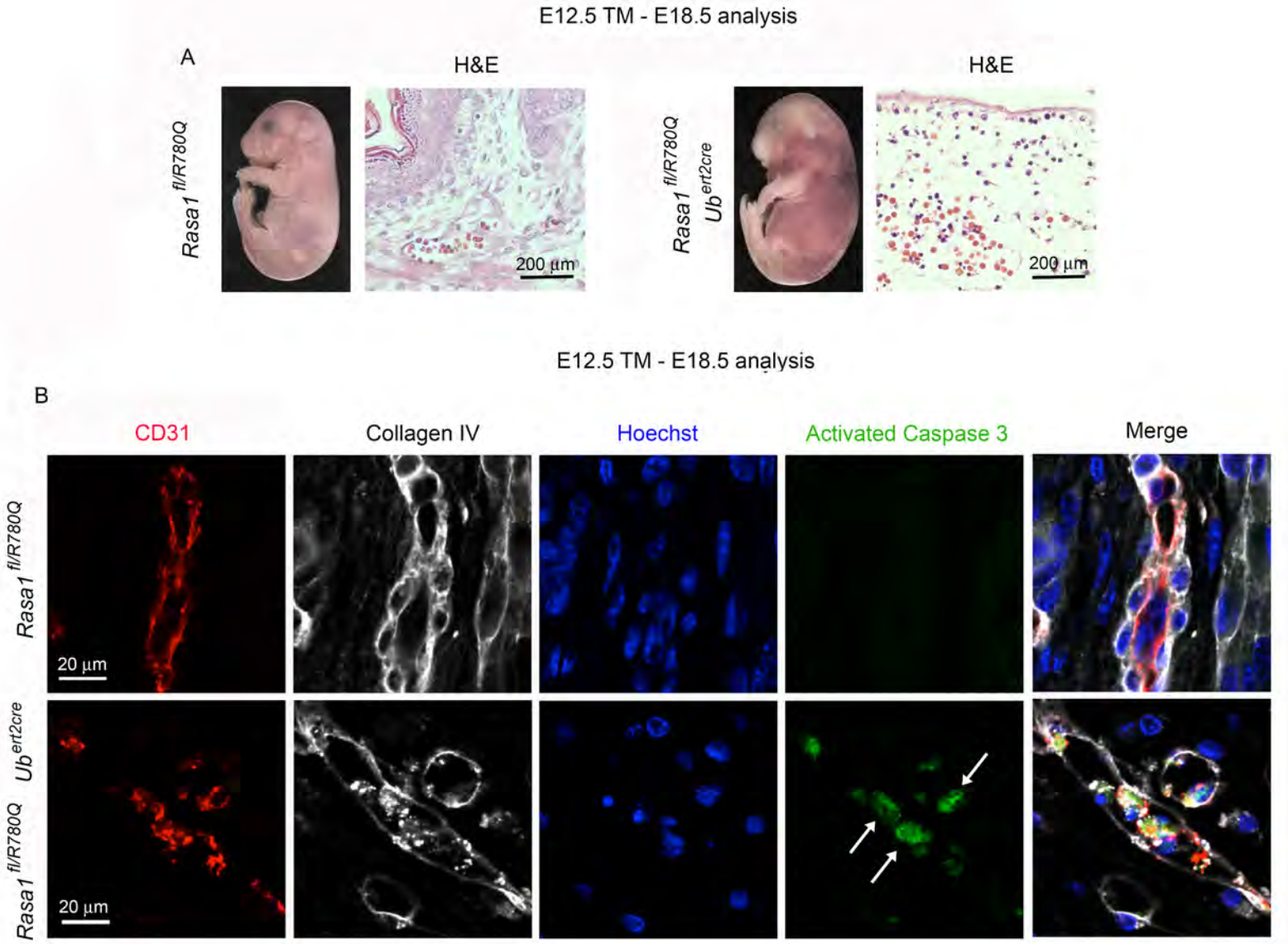

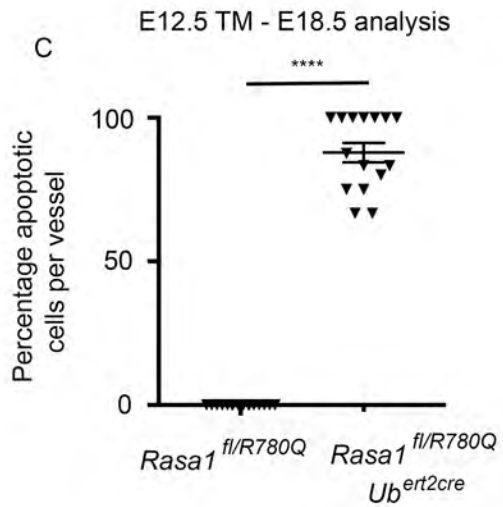

Figure 9. BV abnormalities in embryos induced to express RASA1 R780Q alone during developmental angiogenesis. TM was administered to littermate *Rasa1*$^{fl/R780Q}$ and *Rasa1*$^{fl/R780Q}$ *Ub*^{ert2cre} embryos at E12.5 and embryos were harvested at E18.5. (**A**) Gross appearance of embryos. Note cutaneous hemorrhage in *Rasa1*$^{fl/R780Q}$ *Ub*^{ert2cre} embryos confirmed by H&E staining of skin sections. (**B**) Skin sections were stained with Hoechst and antibodies against collagen IV, CD31 and activated caspase 3. Note discontinuous distribution of collagen IV in BV BM, accumulation of collagen IV in BEC and presence of activated caspase 3 in nuclei of BEC (arrows) of *Rasa1*$^{fl/R780Q}$ *Ub*^{ert2cre} embryos. (**C**) Quantitation of BEC apoptosis in skin BV of *Rasa1*$^{fl/R780Q}$ and *Rasa1*$^{fl/R780}$ *Ub*^{ert2cre} embryos administered TM at E12.5 and harvested at E18.5. Shown is the mean +/- 1 SEM of the percentage of activated caspase 3+ BEC per BV (n=15 BV each genotype). ****, $P<0.0001$, Student's 2-sample t-test.

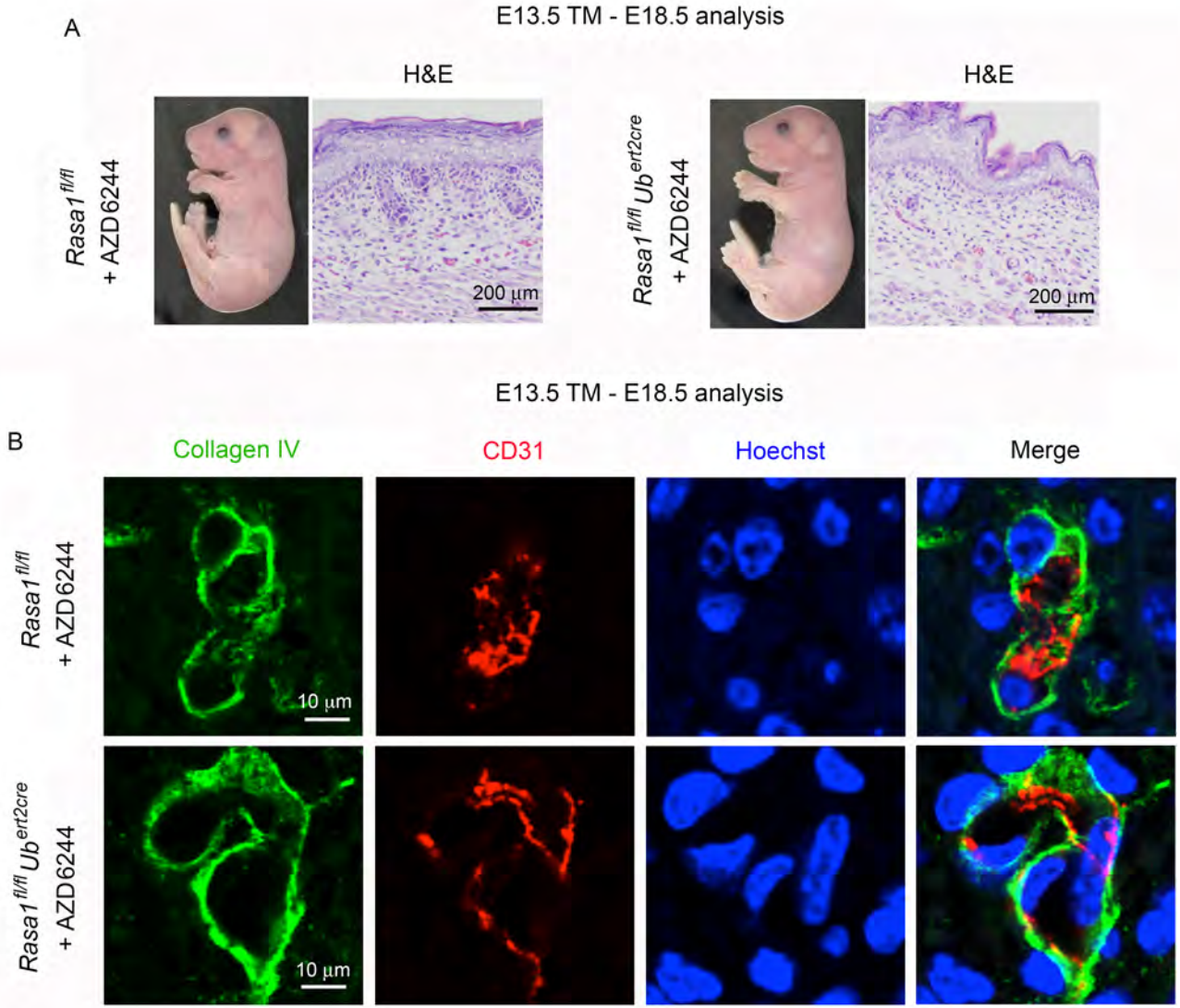

Figure 10. An inhibitor of MAPK signaling blocks the development of BV abnormalities resulting from induced loss of RASA1 during developmental angiogenesis. TM was administered to littermate *Rasa1*$^{fl/fl}$ and *Rasa1*$^{fl/fl}$ *Ub*^{ert2cre} embryos at E13.5. The MAPK pathway inhibitor, AZD6244, was co-administered with the TM and was also administered to embryos on the following two days afterward. Embryos were harvested at E18.5. (**A**) Gross appearance of embryos. Note absence of hemorrhage and edema in *Rasa1*$^{fl/fl}$ *Ub*^{ert2cre} embryos that was confirmed by H&E staining of skin sections. (**B**) Skin sections were stained with Hoechst and antibodies against collagen IV and CD31. Note normal deposition of collagen IV in vascular BM in *Rasa1*$^{fl/fl}$ *Ub*^{ert2cre} embryos.

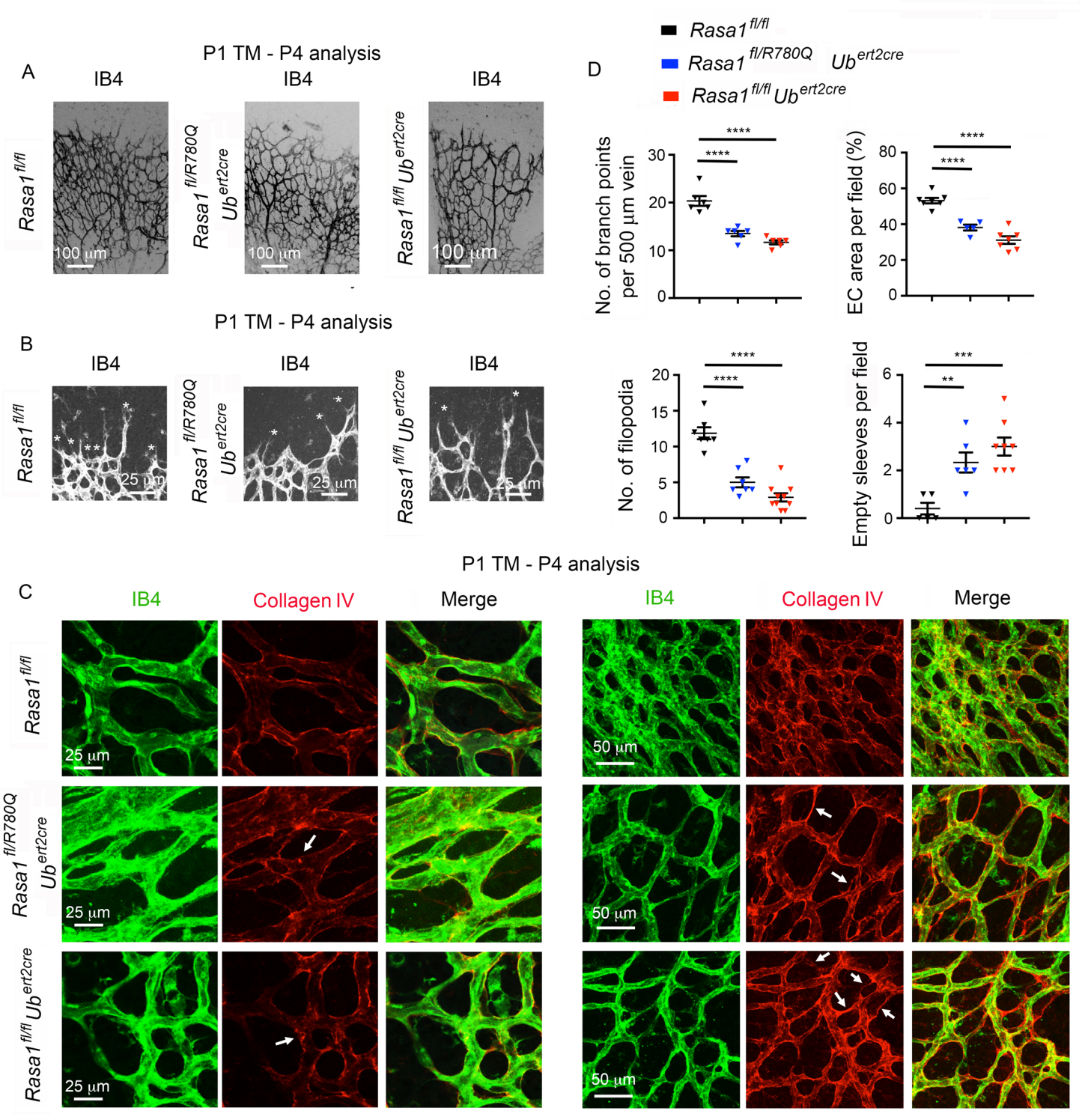

Figure 11. Impaired retinal angiogenesis in neonatal induced RASA1 R780Q and RASA1-deficient mice. TM was administered to littermate *Rasa1*$^{fl/fl}$, *Rasa1*$^{fl/R780Q}$*Ub*^{ert2cre} and *Rasa1*$^{fl/fl}$ *Ub*^{ert2cre} mice at P1 and retinas were harvested at P4. (**A-C**) Retinas were stained with isolectin B4 (IB4) to identify BV and anti-collagen IV (**C**). (**A,B**) Representative low (**A**) and high (**B**) power images of IB4 staining are shown. *, filopodia at the vascular front. (**C**) High power images (left) to show collagen IV accumulation in BEC of *Rasa1*$^{fl/R780Q}$*Ub*^{ert2cre} and *Rasa1*$^{fl/fl}$ *Ub*^{ert2cre} retinas (arrows) and lower power images (right) to illustrate empty collagen IV sleeves in *Rasa1*$^{fl/R780Q}$*Ub*^{ert2cre} and *Rasa1*$^{fl/fl}$ *Ub*^{ert2cre} retinas (arrows). (**D**) Graphs show mean +/- 1 SEM of the number of branch points from veins (n=6 retinas each genotype), the percentage coverage of retinas with BEC per field (n=5-7 retinas each genotype), the number of filopodia per vascular field (n=7-10 retinas each genotype), and the number of empty collagen sleeves per field (n=5-8 retinas each genotype). **, $P<0.01$; ***, $P<0.001$,****, $P<0.0001$, one-way ANOVA test with a Dunnett's multiple comparisons post-hoc test.

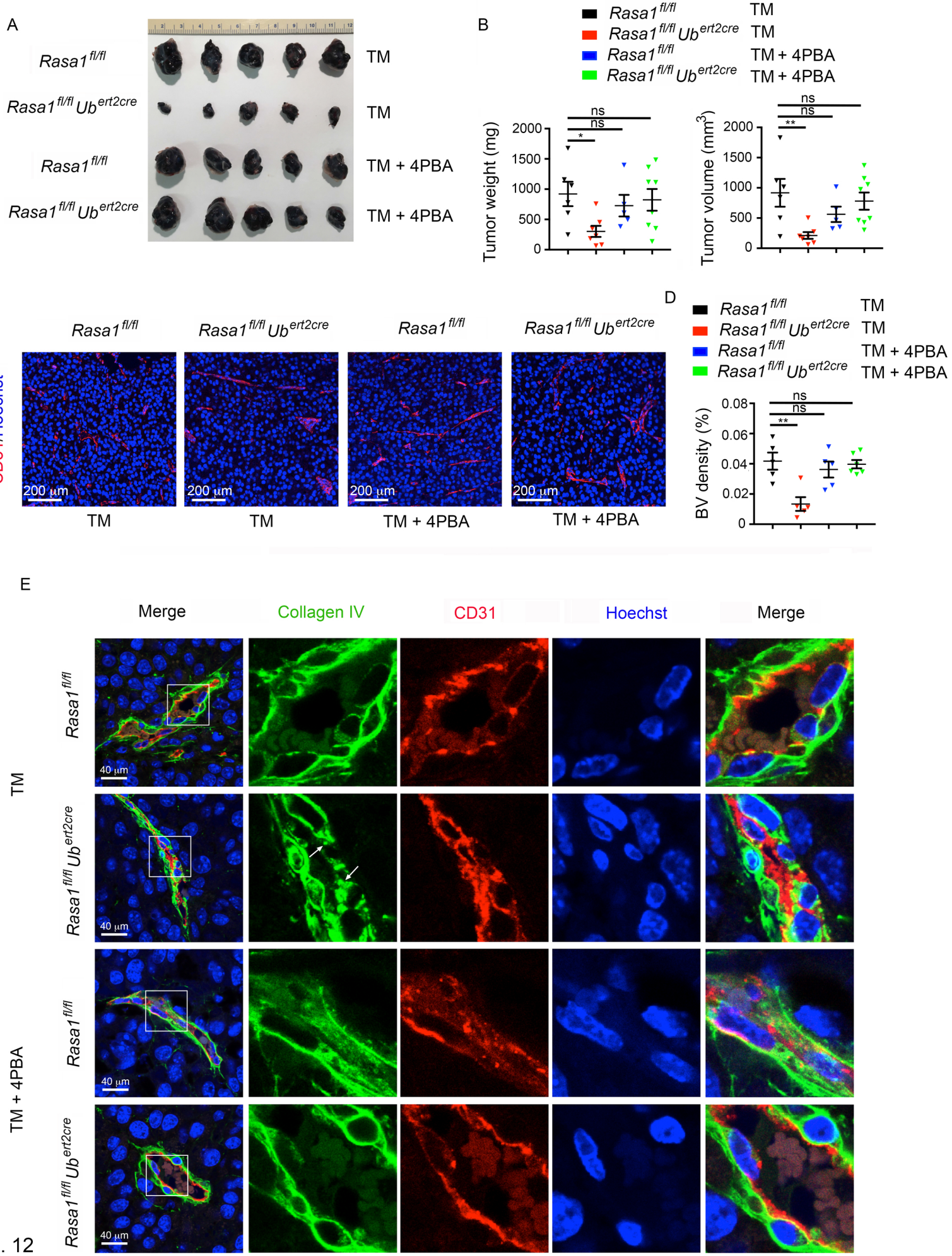
A
Rasa1 fl/fl
Rasa1 fl/fl Ub ert2cre
Rasa1 fl/fl
Rasa1 fl/fl Ub ert2cre
TM
TM
TM + 4PBA
TM + 4PBA
B
Rasa1 fl/fl TM
Rasa1 fl/fl Ub ert2cre TM
Rasa1 fl/fl TM + 4PBA
Rasa1 fl/fl Ub ert2cre TM + 4PBA
Tumor weight (mg)
Tumor volume (mm3)
ns
ns
*
**
C
Rasa1 fl/fl
Rasa1 fl/fl Ub ert2cre
Rasa1 fl/fl
Rasa1 fl/fl Ub ert2cre
CD31/Hoechst
200 μm
TM
TM
TM + 4PBA
TM + 4PBA
D
Rasa1 fl/fl TM
Rasa1 fl/fl Ub ert2cre TM
Rasa1 fl/fl TM + 4PBA
Rasa1 fl/fl Ub ert2cre TM + 4PBA
BV density (%)
E
Merge
Collagen IV
CD31
Hoechst
Merge
TM
TM + 4PBA
Rasa1 fl/fl
Rasa1 fl/fl Ub ert2cre
40 μm

Fig. 12

Figure 12. Disruption of *Rasa1* in adult mice inhibits pathological angiogenesis in a B16 melanoma model. Littermate adult *Rasa1*$^{fl/fl}$ and *Rasa1*$^{fl/fl}$ *Ub*^{ert2cre} mice were administered TM before subcutaneous injection of B16 melanoma cells into flanks one week later. 4PBA was administered to some mice at the same time as B16 melanoma cells and every day thereafter for the duration of the experiment. After 13 days, mice were euthanized and tumors were harvested. (**A**) Representative images of harvested tumors are shown. (**B**) Graphs show mean +/- 1 SEM of tumor weight and volume (n=5-8 tumors from mice of each genotype and treatment condition). (**C**) Sections of tumors were stained with Hoechst and CD31 antibodies. Representative images show reduced BV density in tumors from *Rasa1*$^{fl/fl}$ *Ub*^{ert2cre} mice treated TM alone. (**D**) Graph shows mean +/- 1 SEM of percentage coverage of fields with BV (n=5-6 tumors from mice of each genotype and treatment condition). (**E**) Tumor sections were stained with Hoechst and antibodies against collagen IV and CD31. Representative images are shown. Note accumulation of collagen IV in BEC of tumors from *Rasa1*$^{fl/fl}$ *Ub*^{ert2cre} mice treated with TM alone (arrows). *, $P<0.05$, **, $P<0.01$; ns, not significant, one-way ANOVA test with a Dunnett's multiple comparisons post-hoc test